Master Thesis

Department of Biology - Department of Chemistry
Postgraduate program “Protein Biotechnology”
Molecular Entomology Lab

Immunolocalization study of detoxification enzymes (Cytochrome P450, Glutathione S-Transferase, Intradiol Ring-Cleavage Dioxygenase) in the major agricultural pest *Tetranychus urticae*

Μελέτη ανοσοεντοπισμού ενζύμων αποτοξικοποίησης (Κυτοχρωμικές P450, Μεταφοράσες της Γλουταθειόνης, Διοξυγενάσες) στο Άκαρι *Tetranychus urticae*

Stavrini Papadaki

Scientific Supervisor: Associate Professor John Vontas

Academic Supervisor: Associate Professor Dimitris Tzamarias

List of Figures

Figure 3.15: **Immunolocalization of CYP392A16 using anti-CYP392A16 antibody in 1:250 dilution on whole mount specimens**

Figure 3.16: **Immunolocalization of CYP392A16 using anti-CYP392A16 antibody in 1:250 dilution on whole mount specimens**

List of Tables

Ευχαριστίες

Με την ολοκλήρωση της μεταπτυχιακής μου διατριβής και κατ'επέκταση την ολοκλήρωση του μεταπτυχιακού, θα ήθελα να ευχαριστήσω κάποιους ανθρώπους. Αρχικά, τον κ. Βόντα που με εμπιστεύτηκε και μου έδωσε την ευκαιρία να εργαστώ σε ένα αξιόλογο εργαστήριο. Επίσης, για τη στήριξη και την κατανόηση που έδειξε σε μία δύσκολη περίοδο για μένα.

Στη συνέχεια θα ήθελα να ευχαριστήσω τη Μαρία Ρήγα, "μητέρα" του project αυτού, για τις συμβουλές, τις συζητήσεις, το brainstorming και την καθοδήγηση κατά τη διάρκεια των πειραμάτων. Τη Βασιλεία Μπαλαμπανίδου γιατί έδρασε ως ψύχραιμος και λογικός παρατηρητής κάνοντας απλές αλλά σημαντικές επισημάνσεις. Τέλος, θα ήθελα να ευχαριστήσω τα υπόλοιπα μέλη του εργαστηρίου για τη συνεργασία και την ψυχολογική υποστήριξη και κατανόηση (Τμήμα Βιολογίας, ΙΤΕ). Είναι σημαντικό να ξέρεις ότι δεν είσαι μόνος σου.

Ειδικότερα, τη Νατάσα Καμπουράκη και τη Βασιλεία Μπαλαμπανίδου που στις στιγμές πανικού και απογοήτευσης ήταν εκεί για να προσφέρουν απλόχερα τη βοήθειά τους και τη συμβουλή τους. Επίσης για τα ευχάριστα διαλείμματα από τη δουλειά που υπήρξαν για μένα πηγή δύναμης για να συνεχίσω και πηγή προβληματισμού.

Ένα μεγάλο ευχαριστώ στο σύντροφό μου ο οποίος με στήριζε καθημερινά. Για την υπομονή και την κατανόηση που έδειξε όλο αυτό το χρονικό διάστημα. Θα ήθελα επίσης να ζητήσω συγνώμη από τους φίλους μου που τους παραμέλησα αυτό το διάστημα και ένα τεράστιο ευχαριστώ που δε με ξέχασαν.

Φυσικά δε μπορώ παρά να ευχαριστήσω τους γονείς μου οι οποίοι ήταν δίπλα μου σε όλες τις δύσκολες στιγμές και με την εξαιρετική συμπεριφορά τους έπαιξαν καταλυτικό ρόλο σε κάθε μου βήμα. Δέχτηκαν τις αποφάσεις μου και με στήριξαν παραπάνω απ'όσο χρειαζόταν. Τα λόγια είναι περιττά. Ευχαριστώ!

Abstract

Tetranychus urticae Koch, 1836 is a major agricultural pest that belongs to the Subclass of Acari. It is known for its polyphagous behavior, as it can infest more than 1.100 different plant species, as well as its ability to develop resistance to insecticides/acaricides in very short periods after their first application. Some of its biological characteristics contribute to resistance development such as its high fecundity, haplo-diploid sex determination and short life cycle. Additional characteristics such as its polyphagous behavior have been correlated with the ability of *T. urticae* to counteract the effect of insecticides based on the pre-adaptation theory. The sequencing of *T.urticae* genome further supports this hypothesis since it revealed an extraordinary arsenal of detoxification enzymes, many of which are *T. urticae* specific. Previous studies have shown the over-expression of members of CYP392 family (CYP392A11, CYP392A12, CYP392A16, CYP392D2, CYP392D8, CYP392D10) in resistant strains with CYP392A11 metabolizing the METI insecticides fenpyroximate and cyenopyrafen and CYP392A16 metabolizing the avermectin insecticide abamectin. Additionally, members of GST family (TuGSTd05, TuGSTd10, TuGSTd14) have been found to be over-expressed in resistant strains with TuGSTd05 possibly metabolizing the METI insecticide cyflumetofen. In this study we aimed in localizing three major enzyme families (CYP392A, GSTd, ID-RCD). The first two are of known function and it has been confirmed that their increased presence confers resistance. The third is a newly discovered family in arthropods and constitutes a compelling case of horizontal gene transfer, with its function being unknown. Additionally, there are several documented cases where the function of ID-RCDs has been correlated with digestion or detoxification. We raised 4 different antibodies (anti-CYP392A, anti-CYP392D, anti-GSTd and anti-Dioxygenase) each of which was first tested on Western blot analyses to see their specificity. Three out of four were not specific for the selected subfamily/family (anti-CYP392D, anti-GSTd and anti-Dioxygenase) so we continued the immunolocalization studies with anti-CYP392A and anti-CYP392A16, which were used in cryo-sections and whole mount specimens of *T. urticae* adult females. A part of the results using anti-CYP392A16 indicates the possible presence of A16 in nerve cells proximal to the central nervous mass of *T. urticae*. This finding is in accordance with previously conducted experiments on different organisms such as the mosquito *Aedes albopictus* (Grigoraki et al. 2016), the silkworm *Bombyx mori* (Xuan et al. 2014) and the red floor beetle *Tribolium castaneum* (Zhu et al. 2010). Our efforts should be focused in finalizing the immunolocalization protocol so that our data are consistent, while the co-localization of CPR, the redox partner of CYP392A16, would further support the data.

KEY WORDS: *Tetranychus urticae*, immunolocalization, CYP392, GST, ID-RCDs

Περίληψη

Το είδος *Tetranychus urticae* Koch, 1836 ανήκει στην Υφομοταξία Ακάρεα. Είναι ένα από τα πιο πολυφάγα και καταστροφικά για τις καλλιέργειες αρθρόποδα καθώς προσβάλλει περισσότερα από 1.100 είδη φυτών. Ο τετράνυχος είναι επίσης γνωστός για την ικανότητά του να αναπτύσσει ανθεκτικότητα σε εντομοκτόνα και ακαρεοκτόνα σε πολύ μικρό χρονικό διάστημα μετά την πρώτη τους εφαρμογή. Ορισμένα από τα βιολογικά του χαρακτηριστικά που συνεισφέρουν στην ανάπτυξη της ανθεκτικότητας είναι ο μικρός κύκλος ζωής του, η υψηλή γονιμότητα και ο τρόπος αναπαραγωγής του (αρρενότοκη παρθενογέννεση). Επιπλέον η ικανότητα προσβολής μεγάλου αριθμού φυτών-ξενιστών έχει συσχετιστεί με την ικανότητα του οργανισμού να εξουδετερώνει την επίδραση των εντομοκτόνων, ένας συσχετισμός που γίνεται μέσω της θεωρίας της προ-προσαρμογής. Η αλληλούχιση του γονιδιώματος του τετρανύχου αποκάλυψε ένα εντυπωσιακό οπλοστάσιο ενζύμων αποτοξικοποίησης, εκ των οποίων πολλές οικογένειες παρουσιάζουν μία σύσταση ειδική για τον τετράνυχο. Το γεγονός αυτό επιβεβαιώνει σε ένα βαθμό την υπόθεση της προ-προσαρμογής. Πρόσφατες μελέτες δείχνουν την υπερέκφραση γονιδίων της οικογένειας CYP392 (CYP392A11, CYP392A12, CYP392A16, CYP392D2, CYP392D8, CYP392D10) με την CYP392A11 να έχει δειχτεί ότι μεταβολίζει τα METI εντομοκτόνα fenpyroximate και cyenopyrafen, ενώ η CYP392A16 μεταβολίζει την αβερμεκτίνη abamectin. Επιπροσθέτως, μέλη της οικογένειας GST έχουν βρεθεί ότι υπερεκφράζονται σε ανθεκτικούς πληθυσμούς, ενώ η TuGSTd05 έχει αποδειχθεί ότι μεταβολίζει το METI εντομοκτόνο cyflumetofen. Στη συγκεκριμένη μελέτη στοχεύσαμε στον εντοπισμό τριών μεγάλων οικογενειών ενζύμων (CYP392, GST, ID-RCD) με τη χρήση αντισωμάτων. Οι δύο πρώτες οικογένειες έχουν γνωστή λειτουργία και έχει επιβεβαιωθεί ότι συνεισφέρουν στην ανθεκτικότητα. Η τρίτη οικογένεια πρωτεϊνών ανακαλύφθηκε πρόσφατα στον τετράνυχο και η ακριβής λειτουργία των μελών της είναι ακόμα άγνωστη, αν και έχει συσχετιστεί με την πέψη ή την αποτοξικοποίηση. Για τον εντοπισμό αυτών των οικογενειών τέσσερα αντισώματα σχεδιάστηκαν και παράχθηκαν (anti-CYP392A, anti-CYP392D, anti-GSTd, anti-Dioxygenase). Τα αντισώματα αυτά αρχικά δοκιμάστηκαν με την τεχνική αποτύπωσης κατά Western για να επιβεβαιώσουμε την ειδικότητά τους. Τα τρία από τα τέσσερα αποδείχθηκαν μη ειδικά (anti-CYP392D, anti-GSTd, anti-Dioxygenase), οπότε η μελέτη ανοσοεντοπισμού συνεχίστηκε με τη χρήση του anti-CYP392A και του anti-CYP392A16, ένα ειδικό αντίσωμα για την A16 σχεδιασμένο στο παρελθόν από το εργαστήριο μας. Τα δύο αντισώματα χρησιμοποιήθηκαν σε κρυοτομές ενήλικων θηλυκών ατόμων του οργανισμού καθώς επίσης και σε ολόκληρους οργανισμους (whole mount). Τα αποτελέσματα μας έδωσαν μία ένδειξη σχετικά με τον ιστό στον οποίο εντοπίζεται η A16, όπου φαίνεται να βρίσκεται πιθανοτατα σε κύτταρα του νευρικού ιστού κοντά στο κεντρικό νευρικό σύστημα του τετρανύχου. Παρόμοια αποτελέσματα έχουν βρεθεί και σε μελέτες άλλων οργανισμών όπως το κουνούπι *Aedes aegypti* (Grigoraki et al. 2016), το *Bombyx mori* (Xuan et al. 2014) και το *Tribolium castaneum* (Zhu et al. 2010). Οι προσπάθειές μας πρέπει να προσανατολιστούν στην τελειοποίηση και οριστικοποίηση του πρωτοκόλλου ανοσοεντοπισμού, ενώ η χρήση επιπλέον αντισώματος ειδικό για την κυτοχρωμική P450 αναγωγάση (CPR) μπορεί να επιβεβαιώσει τα μέχρι τώρα αποτελέσματα.

ΛΕΞΕΙΣ ΚΛΕΙΔΙΑ: *Tetranychus urticae*, ανοσοϊστοχημεία, CYP392, GST, ID-RCDs

Contents

1. Introduction

1.1 The two-spotted spider mite *Tetranychus urticae*

Tetranychus urticae Koch, 1836 belongs to the subclass of Acari, family Tetranychidae. It is considered one of the most polyphagous arthropod herbivore species as it can infest more than 1,100 plant species belonging to more than 140 plant families (Migeon and Dorkeld 2010). The two-spotted spider mite feeds on leaf tissues during mobile life stage causing the appearance of chlorotic spots and in prolonged periods of feeding the collapse of the mesophyll layer (Sances et al. 1979, Park and Lee 2002). Regarding its feeding behavior, it has been shown that *T. urticae* is a cell-feeding herbivore, i.e. *T. urticae* penetrates the leaf using its stylet and feeds on mesophyll cell content without a preference in cell type (Bensoussan et al. 2016).

The two-spotted spider mite is considered a generalist and as one, it is challenged with a great variety of plant secondary defense compounds. Its polyphagous nature along with the worldwide distribution of the species has rendered it one of the most important agricultural pests. Important characteristics of its biology include its short life-cycle (Figure 1.1), high fecundity and haplo-diploid sex determination. The aforementioned characteristics have been highly correlated with the ability of the species to develop resistance in various classes of insecticides.

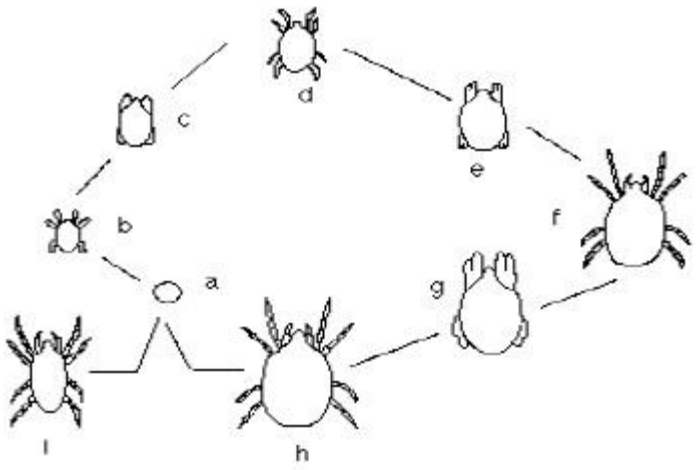

Figure 1.1: Life cycle of *Tetranychus urticae*. The five stages are presented: a. egg, b. larva, d. protonymph, f. deutonymph and h. the adult female. There are three mobile immature stages (larva, protonymph, deutonymph) each followed by a quiescent stage (protochrysalis, deutochrysalis and teliochrysalis). **a.** egg, **b.** larvae, **c.** protochrysalis, **d.** protonymph, **e.** deutochrysalis, **f.** deutonymph, **g.**

teliocrhysalis, **h.** adult female, **i.** adult male. Females are 0.5mm long and males 0.3mm. Under optimum conditions (25^0C) *T. urticae* completes one life cycle in 10-13 days (Van Pottelberge, PhD, 2008).

The recent sequencing of *T. urticae* genome showed a rather compact configuration when compared with other arthropod species regarding gene density, while at the same time it revealed extraordinary instances of gene gains and losses. More specifically it was discovered that gene families which are correlated with digestion, detoxification and transport of xenobiotics were expanded when compared to insects, and presented a unique spider mite-specific composition. Regarding *cytochrome P450* (*CYP*) genes, a total number similar to that of insects was found but with an impressive expansion of intronless *CYP* genes that belong to Clan 2 and are *T. urticae*-specific. Additionally, an expansion was observed in *glutathione S-transferase* (*GST*) genes of delta and mu class, where a total of 12 mu class GSTs was found, a class believed to be vertebrate specific. The sequencing of *T. urticae* genome revealed also the existence of gene families that had not been reported so far in metazoan species. These include the intradiol ring-cleavage dioxygenases (ID-RCDs), a family found mostly in bacteria and fungi (Vaillancourt et al. 2006, Grbíc et al. 2011). The 16 annotated functional genes of this family present high sequence similarity with the homologue of *Streptomyces avermitilis* suggesting a case of horizontal gene transfer (Grbić et al. 2011).

T. urticae has a great ability to develop resistance to many different classes of insecticides/acaricides in a very short period after their use (Knowles 1997, Van Leeuwen et al. 2008), while cross-resistance of *T. urticae* populations has also been documented (Nicastro et al. 2010, Sugimoto and Osakabe 2014). This has been attributed to biological characteristics of the species, such as those mentioned before, although the exact genetic basis of resistance is not yet fully understood (Khajehali et al. 2011). Nevertheless, significant progress has been made towards this direction (reviewed in Van Leeuwen et al. 2016).

Due to its ability to develop resistance rapidly, *T. urticae* has been characterized as “the most resistant species in terms of the number of pesticides to which populations have become resistant” (Van Leeuwen et al. 2009). Table 1.1 shows a comparison among different arthropod species regarding the number of compounds that resistance has been reported along with the total cases of resistance (Sparks and Nauen 2014), supporting the abovementioned statement.

Table 1.1: Top 10 resistant arthropod species are presented along with the documented resistant cases in unique active ingredients indicating that *T.urticae* is the most resistant arthropod species (Sparks and Nauen 2014).

Species	Common name	Order	No. of compounds	No. of cases
Tetranychus urticae	Two-spotted spider mite	Acari	93	414
Plutella xylostella	Diamondback moth	Lepidoptera	91	576
Myzus persicae	Green peach aphid	Hemiptera	75	402
Musca domestica	House fly	Diptera	58	303
Bemisia tabaci	Sweet potato whitefly	Hemiptera	54	555
Leptinotarsa decemlineata	Colorado potato beetle	Coleoptera	54	279
Aphis gossypii	Cotton aphid	Hemiptera	48	231
Panonychus ulmi	European red mite	Acari	48	197
Helicoverpa armigera	Cotton bollworm	Lepidoptera	47	692
Boophilus microplus	Southern cattle tick	Ixodida	44	167
Blattella germanica	German cockroach	Blattodea	43	219
Spodoptera litura	Mediterranean climbing cutworm	Lepidoptera	38	457

Several approaches have been adopted over the years for the control of *T. urticae* populations aiming in the limitation of damage in economically important crops such as vegetables, fruits, cotton, maize, as well as in various ornamentals. The less common practice, although effective under greenhouse conditions, includes the biological control of the species, were natural enemies of *T. urticae* are introduced. These natural enemies include predatory mites that belong to the Phytoseiidae family [*Phytoseiulus macropilis* (Gigon et al. 2016), *Neoseilius californicus* (Fraulo and Liburd 2007)] as well as species that belong to the class Insecta [*Stethorous punctilum* (García-Marí and Gonzáles-Zamora 1999), *Macrolophus pigmeus* (Gigon et al. 2016)].

The most common approach for controlling *T. urticae* populations in field crops has been the use of insecticides or specific acaricides. These chemical compounds include avermectins while Mitochondrial Electron Transport Inhibitors (METIs) have been more recently introduced. Each class of these compounds presents a different chemical structure as well as a different mode of action (Knowles 1997, Dekeyser 2005, Van Leeuwen et al. 2009).

1.2 Insecticide classes and their mode of action

The application of insecticides and acaricides, as mentioned in section 1.1, is the most common approach for controlling *T.* urticae populations in field crops. Over the years different classes of chemical compounds have been used such as organophosphates and pyrethroids which act on both insects and acari. Furthermore, the action of the insecticide/acaricide could

be life-stage specific [fenpyroximate (METI): all stages, hexythiazox (Mite Growth Inhibitor): eggs, immature stages), while the vast majority of insecticides target on muscle or nervous system such as pyrethroids and macrocyclic lactones. In this project we will focus on avermectins, a repeatedly used insecticide class, and METIs, the recently introduced inhibitors of the electron transport chain in mitochondria.

Avermectins consist an important class of insecticides with several cases of resistance being documented (Ghosh et al. 2012, Zhang et al. 2013, Riga et al. 2014, Mermans et al. 2017). Avermectins are macrocyclic lactones produced from the fermentation process of the soil microorganism *Streptomyces avermitilis* (Clark et al. 1994). They act on glutamate-gated chloride channels (GluCl) of insects and acari. The binding of these compounds to the GluCl channel is irreversible, keeping the channel in the open conformation thus preventing the physiological function of these proteins (Wolstenholme and Rogers 2005). The final effect upon the target organism is paralysis. Avermectins are also used as antiparasitic drugs in veterinary medicine and livestock farming (McKellar and Benchaoui 1996), beside their use for controlling agricultural pests (Putter et al. 1981).

Mitochondrial electron transport inhibitors (METIs) have been introduced in agricultural pest management since the early 1990s. The first compounds that were introduced, although they were chemically unrelated, they shared the same mode of action, i.e. inhibition of the complex I of the electron transport chain in mitochondria (Hollingworth et al. 1995). More specifically, the function of NADH:ubiquinone oxidoreductase is inhibited and the translocation of protons from NADH to ubiquinone is hindered (Lümmen 2007). Recently, other chemical compounds became available which inhibit the complex II of the electron transport chain (Yu et al. 2012, Hayashi et al. 2013) inhibiting succinic dehydrogenase. In some cases it has been shown that the chemical compounds that share this general mode of action (METIs) present very low toxicity against other organisms as beneficial insects and vertebrates (Hayashi et al. 2013).

1.3 Insecticide resistance and resistance mechanisms

Insecticide resistance can be defined as “a heritable phenomenon where the susceptibility of a population to a toxin decreases after the repetitive exposure of the population to the toxin for several generations” (Heckel 2012) (Figure 1.2). An alternative definition of the phenomenon is provided by the Insecticide Resistance Action Committee (IRAC) according to

which insecticide resistance is a heritable change in the sensitivity of a pest population that is reflected in the repeated failure of a product to achieve the expected level of control when used according to the label recommendation for the pest species.

The basic idea behind insecticide resistance development in a population is that a difference in the genetic background of a small part of the population offers an evolutionary advantage upon insecticide application and thus these individuals have higher possibilities in surviving and reproducing. This way, and after repetitive exposure of the population to the same active compound for several generations (selective pressure), the frequency of the trait conferring resistance is increased in the population and finally established (Brattsten et al. 1986). In the case of *T. urticae*, it has been proposed that the evolutionary history of the species that led to its ability to feed on a wide range of host plants, and thus become exposed to a variety of plant allelochemicals, has resulted in pre-adaptation to several classes of insecticides. This hypothesis has long been proposed and still remains under debate (Gordon 1961, Croft and Stickler 1983, Rosenheim et al. 1996), although recent molecular data support it (Dermauw et al. 2013).

The development of resistance is a complex biological phenomenon and many factors could contribute to the final resistant phenotype. These factors could be divided in four categories, each representing a different mechanism of resistance development. The first line of defense against chemical compounds is behavioral resistance where the individuals develop behaviors through which the exposure to the insecticide is reduced (Sparks et al. 1989). The aforementioned behaviors include reduced activity (motility/feeding) of the individuals that affect the contact with insecticide residues as well as alterations in host/habitat preferences. Recently this resistance mechanism was characterized as behavioral avoidance rather than behavioral resistance (Zalucki and Furlong 2017). This shift in terminology is attributed basically to the lack of evidence regarding the existence of biological traits that could lead to behavioral changes and finally behavioral resistance. Although, in some cases, a correlation between taste/odor receptors and behavioral resistance has been documented (Hostetler et al. 1994), in other cases the existence of behaviors contributing to resistance could be appointed to behavioral plasticity in an altered environment (Govella et al. 2013). A characteristic example of insecticide with repellent properties is the class of pyrethroids (Lockwood et al. 1985, Russell et al. 2011).

Another resistance mechanism to insecticides is cuticle resistance. Cuticle resistance is defined as the reduced ability of the insecticide to reach the hemolymph due to decreased penetration. Decreased penetration has been attributed to increased thickness of the cuticle through increased secretion of lipids, chitin and hydrocarbons (Plapp and Hoyer 1968, Juarez

and Fernandez 2007, Balabanidou et al. 2016, Yahouédo et al. 2017). Although this mechanism of resistance has not been thoroughly investigated, during the past years significant progress has been made towards understanding and deciphering its complexity (Pignatelli et al. 2017, Yahouédo et al. 2017, Seixas et al. 2017, Dank et al. 2017, Zhou et al. 2017).

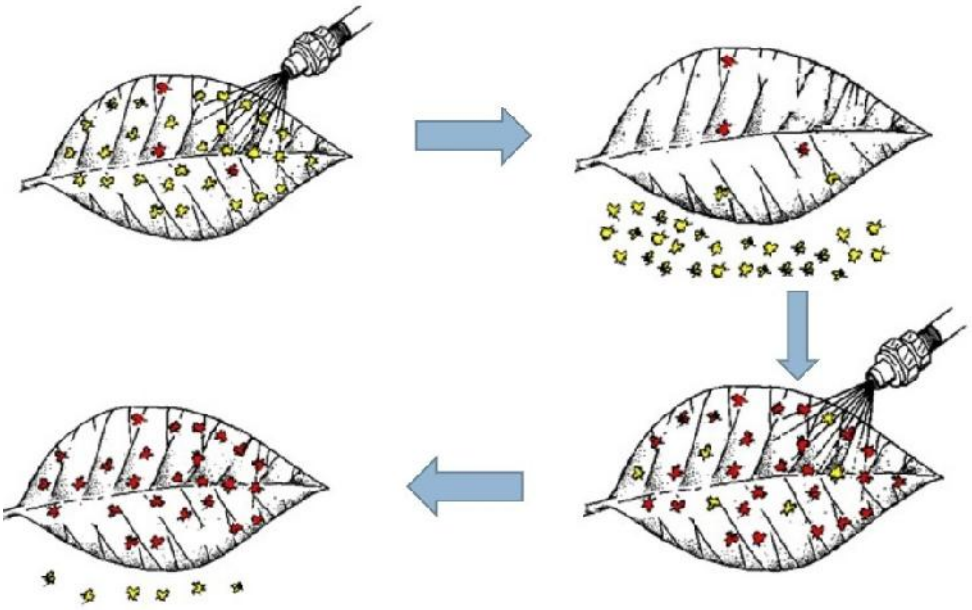

Figure 1.2: Resistance as a heritable phenomenon. Yellow: susceptible, red: resistant. As it is indicated, the repetitive selection through insecticide application can lead to establishment of resistance-related traits in the population (Pedigo 1989).

The third and one of the most studied mechanisms of resistance along with metabolic resistance, is target site (or toxicodynamic) resistance. In this case, a modification of the target molecule through mutation(s) in the coding sequence of a protein, results in an altered 3D structure at the target site or reduced affinity of the molecule with the insecticide and finally reduced binding of the insecticide (Feyereisen et al. 2015, Van Leeuwen et al. 2016). Several studies have shown the existence of point mutations that lead to amino acid substitutions and their direct correlation with increased resistance levels in many organisms. Voltage-gated sodium channel is a characteristic example where point mutations in various species confer elevated levels of resistance to pyrethroids [*Anopheles gambiae* (Jones et al. 2012), *Myzus persicae* (Martinez-Torrez et al. 1999), *Plutella xylostella* (Sonoda et al. 2008), *Tuta absoluta* (Haddi et al. 2012), *Musca domestica* (Williamson et al. 1996), *Tetranychus urticae* (Tsagkarakou et al. 2009)], while Glutamate-gated Chloride channel (GluCl) mutations have

been shown to confer resistance to avermectins [*Tetranychus urticae* (Kwon et al. 2010) (Dermauw et al. 2012), *Drosophila melanogaster* (Kane et al. 2000)].

Metabolic (or toxicokinetic) resistance is the last and most well documented mechanism of resistance. It refers to the ability of the organism to convert toxic compounds (in this case insecticides) to a more soluble and less toxic form (phase I enzymes) with their subsequent sequestration/conjugation (phase II enzymes) and excretion from the cell (phase III enzymes) (Perry et al. 2011). Three major enzyme families that have been repeatedly shown to be involved in this process are cytochrome P450 mono-oxygenases (CYP450) (phase I) [*Drosophila melanogaster* (Daborn et al. 2002), *Bemisia tabaci* (Karunker et al. 2008), *Plutella xylostella* (Bautista et al. 2009), *Myzus persicae* (Puinean et al. 2010), *Anopheles gambiae* (Nikou et al. 2003)], carboxylesterases (CCE) (phase I enzymes) [*Nilaparvata lugens* (Small and Hemingway 2000), *Musca domestica* (Zhang et al. 2007), *Aphis gossypii* (Cao et al. 2008)] and glutathione S-transferases (GST) (phase II enzymes) [*Anopheles gambiae* (Ranson et al. 2001), *Nilaparvata lugens* (Vontas et al. 2002), *Musca domestica* (Wei et al. 2001), *Aedes aegypti* (Lumjuan et al. 2005), *Anopheles gambiae* (Wang et al. 2008)]. In most cases of metabolic resistance one or several genes encoding the abovementioned enzymes have been found to be over-expressed. The exact mechanism of over-expression is not yet fully understood but in several cases gene amplification (Puinean et al. 2010, Grigoraki et al. 2015) and mutation on *cis*- and *trans*-regulatory elements have been reported (reviewed in Feyereisen et al. 2015). Finally, another factor regarding detoxification enzymes that has been found to contribute to the development of resistance is the alteration of their activity due to amino acid substitutions (Campbell et al. 1998, Cui et al. 2011).

1.4 Cytochrome P450 monooxygenases

Cytochrome P450 genes (or *CYP* genes) constitute one of the largest gene families with representatives in a wide range of organisms including bacteria, protists, fungi, plants and animals (Werck-Reichhart and Feyereisen 2000). The proteins that are encoded by these genes are usually 45-55kDa and they share a common characteristic: they all are heme-thiolate enzymes. These enzymes acquired their name (CYP450) by the characteristic absorbance peak at 450nm that results from their Fe^{II}-CO complex (Omura and Sato 1964). P450s have the ability to catalyze a wide range of reactions (hydroxylation, epoxidation, N-, O-, S-dealkylation), perhaps over 60 different chemical reactions, leading Coon et al. (1996) to call them

diversozymes. Although P450s are characterized as mixed-function oxidases, they are mostly known for their mono-oxygenase activity, catalyzing the transfer of one atom of molecular oxygen to a substrate (S) and reducing the other to water, as described in reaction (1):

$$S + O_2 + NADPH + H^+ \rightarrow SO + H_2O + NADP^+ \qquad (1)\ \text{(Feyereisen 1999)}$$

The nomenclature of P450s was revised in the mid '90s where a CYP prefix is used for all P450s, followed by an Arabic numerical that designates the family, a capital letter that designates the subfamily and another Arabic numerical designating the individual gene (e.g. *CYP4U2*) or transcript and protein (e.g. CYP4U2) (Figure 1.3) (Nebert 1991, Nelson et al. 1993, Nelson et al. 1996). The members of the same family share more than 40% identity, while the members of the same subfamily over 55% identity. In the basis of phylogeny, Nelson suggested the grouping of phylogenetically related CYP proteins into clans (Nelson 1998). From this categorization 4 clans were generated: Clan 2, Clan 3, Clan 4 and mitochondrial clan.

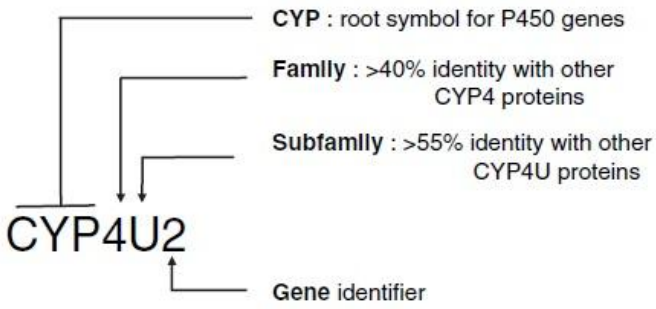

Figure 1.3: Scheme of the P450 nomenclature (Feyereisen 2012).

P450 monooxygenases are either microsomal or mitochondrial and can be divided in 4 categories depending on how the electrons from NAD(P)H are delivered into the catalytic site. Class I proteins require both FAD-containing reductase and iron-sulfur redoxin. Class II proteins are the most studied. They are involved in a series of reactions and pathways, usually in the biosynthesis of hormones (Feyereisen 2012). The proteins that belong to class II P450s have also been implicated in metabolic resistance to insecticides as well as xenobiotic detoxification. They are ER-bound molecules and they require only a FAD/FMN-containing P450 reductase for transfer of electrons. On the other hand, class III enzymes are self-sufficient and do not require an electron donor, while class IV enzymes receive electrons directly from NAD(P)H (Werck-Reichhart and Feyereisen 2000). Figure 1.4 shows the primary structures of P450 proteins that

are either microsomal or mitochondrial, indicating conserved motifs as well as similarities and differences in the primary structure.

A great number of eukaryotic P450s are microsomal (ER-bound) and contain a series of 20 hydrophobic residues followed by a few charged residues. The charged residues act as a halt-transfer signal which is followed by a short motif of prolines and glycines (PPxP). The halt-transfer signal and the proline motif form a “hinge” that keeps the globular domain of the protein on the surface of the membrane, while the N-terminus is anchored through it (Feyereisen 2012). The first conserved motif, WxxxR, is located in helix C and it is believed to form a charged pair with the propionate of the heme. The second motif is located in helix I (GxE/D**T**T/s) and surrounds a conserved threonine. The third motif (ExLR) which is located in helix K is thought to stabilize the overall structure of the protein through interactions with the fourth conserved motif (PxxFxPE/DRF). The heme-binding loop represents the fifth and most conserved structural motif and indicates a common mechanism of electron and proton transfer as well as oxygen activation. This motif is represented by the consensus sequence FxxGxRx**C**xG with the conserved cysteine serving as a fifth ligand to the heme-iron (Werck-Reichhart and Feyereisen 2000, Feyereisen 2012). The most variable regions are correlated with membrane anchoring through the N-terminal of the molecule as well as regions relative to substrate binding and recognition (substrate binding sites, SBSs) (Gotoh 1992).

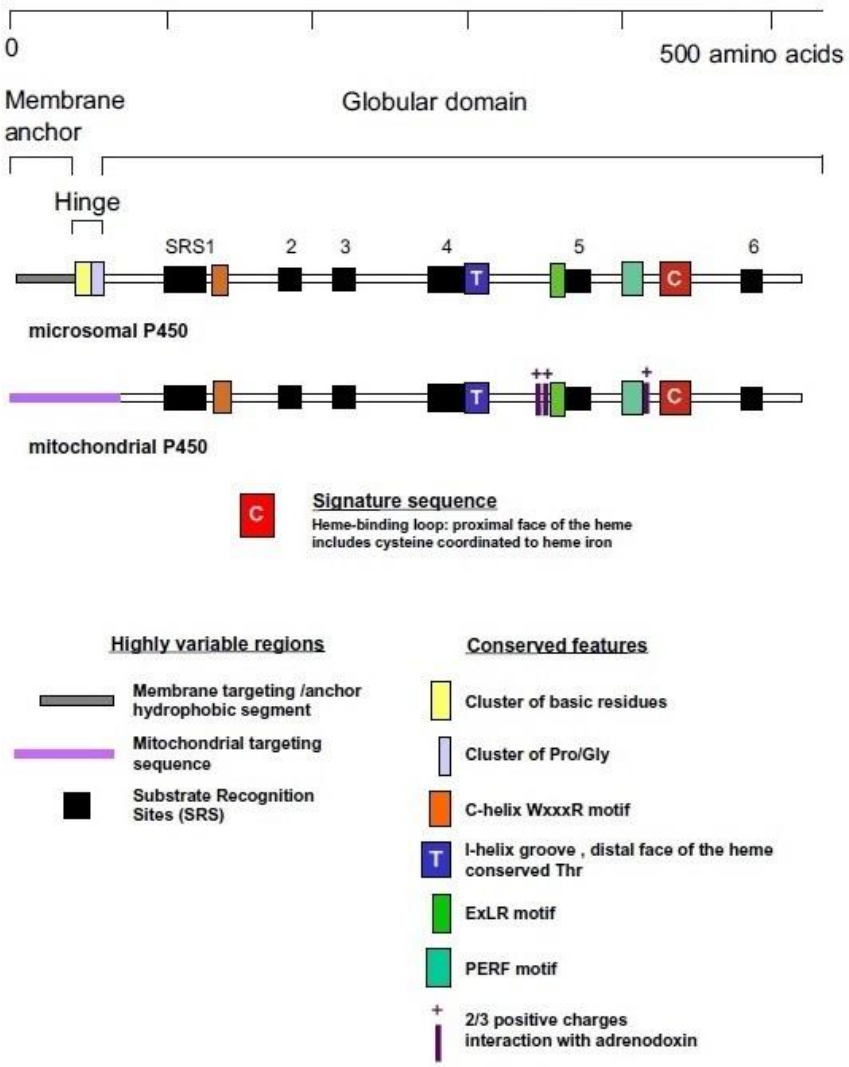

Figure 1.4: Primary structures of P450 proteins. Conserved and variable regions of P450 enzymes are presented (Feyereisen 2012).

1.4.1 *Tetranychus urticae*

The recently sequenced genome of *Tetranychus urticae* revealed a total of 86 *CYP* genes, a number similar to other arthropods. A remarkable expansion of duplicated *CYP2* clan genes was revealed (Table 1.2) and it is believed to be lineage-specific. These genes are intron-less and it has been shown that specifically the family CYP392, which belongs to CYP2 clan, responds highly to acaricide selection and feeding on different hosts. More specifically, CYP392A16 was found to be overexpressed severalfolds in the resistant strains Mar-ab and MR-VP along with other members of CYP392 family, such as CYP392D8, CYP392D10 and

CYP392D2, through whole genome microarray analysis and further confirmation by real-time PCR (Dermauw et al. 2013). Furthermore, the metabolism of abamectin by CYP392A16 was confirmed through metabolism assays of the functionally expressed recombinant protein (Riga et al. 2014).

Additionally, CYP392A11 and CYP392A12 have been found to be overexpressed in METI resistant strains through genome-wide expression data and the ability of CYP392A11 to directly metabolize fenpyroximate (complex I inhibitor) and cyenopyrafen (complex II inhibitor) have been confirmed by metabolism assays (Khalighi et al. 2015, Riga et al. 2015 respectivelly).

Table 1.2: CYPome size of several arthropod species. Approximate total number of CYP genes and numbers of CYP genes per CYP clan (Feyereisen 2012).

	CYPome Size	*CYP2 Clan*	*mitochondrial CYP Clan*	*CYP3 Clan*	*CYP4 Clan*
Insecta					
Drosophila melanogaster	88	7	11	36	32
Anopheles gambiae	105	10	9	40	46
Aedes aegypti	160	12	9	82	57
Culex quinquefasciatus	170				
Bombyx mori	85	7	12	30	36
Apis mellifera	46	8	6	28	4
Nasonia vitripennis	92	7	7	48	30
Camponotus floridanus	132				
Harpegnathos saltator	93				
Tribolium castaneum	134	8	9	72	45
Acyrthosiphon pisum	64	10	8	23	23
Pediculus humanus	36	8	8	11	9
Crustacea					
Daphnia pulex	75	20	6	12	37
Acari					
Tetranychus urticae	86	48	5	10	23

1.5 Glutathione S-Transferases (GSTs)

Glutathione S-transferases constitute a large family of enzymes and they are found in most aerobic eukaryotes and some prokaryotes (Wilce and Parker 1994). They are involved in the detoxification of both endogenous and xenobiotic compounds including insecticides, while

they have also been involved in the sequestration or transport of endogenous hydrophobic compounds (Salinas et al. 1999). In mammals they have been widely studied as they are important in cancer epidemiology and drug resistance (Tew 1994, Hayes and Pulford 1995). The basic reaction that GSTs catalyze is the conjugation of electrophilic compounds with the thiol group of the tripeptide glutathione. This reaction results in a molecule which is more water soluble and excreted more easily than the non-GSH substrate (Habig et al. 1974).

In mammals three major groups of GSTs have been reported, microsomal, cytosolic and mitochondrial. In arthropods no mitochondrial GSTs have been found, while the cytosolic GSTs have been divided in six classes (delta, theta, omega, sigma, epsilon and zeta). The classes delta and epsilon have been linked with insecticide resistance in insects (Enayati et al. 2005, Feyereisen et al. 2015). In addition, Acari contain several genes of mu-class GSTs which until recently were thought to be vertebrate specific (Grbíc et al. 2011, Reddy et al. 2011).

The cytosolic GSTs are usually homo- or hetero-dimers with molecular weight of approximately 25kDa (monomer). The general structure of each monomer consists of two domains that are joined by a linker region. The N-terminal domain constitutes the glutathione binding site (G-site) and spans from residues 1-80, while the serine at position 11 (S11) is known to play a catalytic role in delta class GSTs (Winayanuwattikun and Ketterman 2005). The much larger C-terminal domain consists of alpha helices and contains the hydrophobic ligand binding site (H-site).

1.5.1 *Tetranychus urticae*

GSTs have been implicated in several cases of resistance including *Aedes aegypti* (Lumjuan et al. 2011), *Plutella xylostella* (Zhang et al. 2017) and *Bemisia tabaci* (He et al. 2018), with class delta and epsilon being involved more often in resistance cases in insects. The two-spotted spider mite contains a total of 31 glutathione S-transferase genes, 16 of which belong to class delta and 12 to mu class, while no epsilon GSTs were identified (Grbíc et al. 2011). In *T. urticae* the overexpression of TuGSTd10 and TuGSTd14 has been correlated with resistance in multi-resistant strains as indicated by microarray-based transcriptional studies (Dermauw et al. 2013). Further biochemical analyses revealed that TuGSTd14 enzyme activity is inhibited by the presence of abamectin as the insecticide binds to regions adjacent the active site (Pavlidi et al. 2015). So far, there is no certain conclusion regarding the role of these two in resistant strains of *T. urticae*. Furthermore, Khalighi et al. conducted synergism assays in a

resistant strain of *T. urticae* where it was found that GSTs could play a role in METI detoxification (Khalighi et al. 2014). When the genome-wide gene expression profile of a resistant strain was compared to the parental susceptible strain, TuGSTd05 was identified as a potential candidate conferring resistance. Further computational and biochemical analyses revealed that TuGSTd05 could possibly metabolize the complex II inhibitor cyflumetofen (Pavlidi et al. 2017).

1.6 Intradiol Ring-Cleavage Dioxygenases (ID-RCDs)

Ring-cleavage dioxygenases constitute a family of enzymes found mostly in fungi and bacteria where they play a crucial role in the degradation of aromatic compounds (Vaillancourt et al. 2008). They are divided in two classes, extradiol and intradiol ring-cleaving enzymes, which do not present any sequence or structural similarity, a fact that led to the conclusion that these two classes are evolutionary distinct. Further structural and sequence analyses of the intradiol class showed that all intradiol dioxygenases characterized to date belong to a single evolutionary lineage (Vetting and Ohlendorf 2000, Vaillancourt et al. 2008).

As mentioned above, these classes of enzymes cleave the aromatic nucleus of aromatic compounds by utilizing non-heme Fe (III or II). Intradiol-ring cleavage dioxygenases utilize non-heme Fe (III) to cleave the aromatic nucleus *ortho* to (between) the hydroxyl substituents, while extradiol-ring cleavage dioxygenase urtilize non-heme Fe (II) to cleave the aromatic nucleus *meta* to (adjacent) the hydroxyl substituents. In both cases, the final product of each reaction is further transformed into intermediates of the tricarboxylic acid cycle (TCA) (reviewed in Vaillancourt et al. 2008).

1.6.1 *Tetranychus urticae*

The first report regarding the presence of intradiol-ring cleavage dioxygenases in metazoan species was in 2011 with the sequencing of the genome of the polyphagous spider mite *Tetranychus urticae*. The genome of *T. urticae* contains 16 functional genes of ID-RCDs that present 43% sequence similarity with the homologue of *Streptomyces avermitilis* and share the conserved 2 His 2 Tyr non-heme iron (III). These facts led to the assumption that these genes constitute a compelling case of horizontal gene transfer (Grbíc et al. 2011).

Additionally, Grbíc and his colleagues proposed the involvement of ID-RCDs in digestion or detoxification based on the sequence similarity and the presence of conserved motifs among *T. urticae* ID-RCDs and *S. avermitilis* ID-RCDs (Grbíc et al. 2011). This hypothesis was further tested by Dermauw and his colleagues where they compared transcriptional data from a susceptible and a resistant strain of *T. urticae* (fed on bean plants), as well as transcriptional data from the susceptible strain fed on bean plants and the same strain fed on tomato plants (host-plant change). The results showed a significant overexpression of members of the ID-RCD family both in the resistant strain as well as in the susceptible strain after host-plant change (Dermauw et al. 2013). The genes that were overexpressed included tetur13g04550, tetur28g01250 and tetur01g00490. Furthermore, signal peptide analyses revealed that the members of the ID-RCD family are excreted proteins and present common features with an ID-RCD of *Aspergillus fumigatus* leading the researchers to hypothesize that some *T. urticae* ID-RCDs could recognize and cleave more complex structures than cathecholic substances (Dermauw et al. 2013).

The exact role of ID-RCDs in *T. urticae* has not yet been deciphered but recent findings further support the hypothesis of the involvement of ID-RCDs in digestion or detoxification. Bryon and her colleagues compared the genome-wide expression profiles of *T. urticae* strains under normal conditions and during diapause. Diapause is considered an adaptation that allows mites and insects to survive unfavorable conditions. During this period the metabolism is suppressed, the behavior of the organism changes while it presents high tolerance to stress. Diapausing mites do not reproduce and do not feed. The results of this comparison showed that this family of enzymes was greatly influenced by diapause. Eleven out of 16 genes were differentially expressed, with the vast majority of them (10 out of 11) being down-regulated, strongly suggesting their involvement in digestion or detoxification (Bryon et al. 2013).

1.7 Anatomy of Tetranychus urticae

Tetranychus urticae belongs to the Phylum of Arthropoda, Subclass Acari. The size of the female is approximately 0.5mm long with its body being divided in two parts: the gnathostoma and the idiosoma. The gnathostoma contains the mouthparts which are a set of pedipalps and chelicerae as well as the oral cavity. The gnathostoma is not considered the head of mites as it does not contain neither the eyes nor the “brain” of the mite. On the other hand, the idiosoma is the remainder of the body and consists of the head, the thorax and the abdomen

which in the case of Acari are fused. *Tetranychus urticae* has four pairs of legs while setae are found scattered throughout its body. Setae are sense organs that assist the central nervous system in obtaining information about the environment. Along the body of *T. urticae* mechanosensory and chemosensory setae are found, although the location of each sensory neuron and its exact function is not clear (Bostanian and Morisson 1973, Mills 1973).

A few general characteristics of the internal anatomy of *Tetranychus urticae* include the absence of a circulatory system as well as the absence of connective tissue. The haemocoel is represented by narrow spaces, thus allowing the organs to move against each other (Helle and Sabelis 1985).

1.7.1 Nervous system

The information that we have concerning the nervous system of *T. urticae* is limited. The first one to describe the anatomy of the nervous system was Blauvelt in 1945 and since then little information was added to our knowledge. The central nervous mass in the two-spotted spider mite is called syngaglion and consists of the fused supraoesophageal and suboesophageal gaglia. The relatively large syngaglion lies close to the ventral body surface and it is surrounded by the silk gland, dorsal podocephalic gland, midgut and in females the ovary (Figure 1.5). The oesophagus passes through the central nervous mass (syngaglion) and divides it into a dorsal supraoesophageal mass and a ventral suboesophageal mass (Blauvelt et al. 1945).

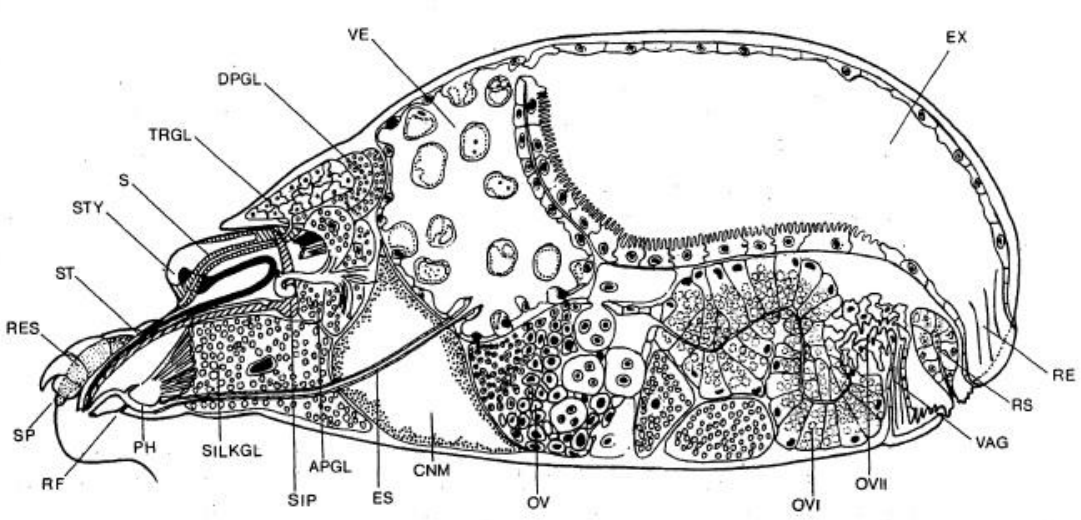

Figure 1.5: Schematic representation of a longitudinal section of a female *T. urticae*. **APGL**: Anterior podocephalic gland, **CNM:** Central nervous mass, **DPGL**: Dorsal podocephalic gland, **ES**: oesophagus,

EX: Excretory organ, **OV**: Ovary, **OVI and OVII**: Anterior and posterior oviduct, **PH**: Pharyngeal pump, **RE**: Rectum, **RES**: Reservoir of silk glands, **RF**: Rostral fossette, **RS**: Receptaculum seminis, **S**: Septum inside stylophore, **SIP**: Sigmoid piece, **SILKGL**: Silk gland, **SP**: Spinerrete, **ST**: Stylet, **STY**: Stylophore, **TRGL**: Tracheal gland, **VAG**: Vagina, **VE**: Ventriculus (Helle and Sabelis 1985).

1.7.2 Digestive system

The digestive system consists of the foregut, the midgut and hindgut. Mouth, pharynx and oesophagus comprise the foregut, ventriculus and coecae comprise the midgut and excretory organ, rectum and anus comprise the hindgut. Regarding the midgut, the ventriculus is located immediately behind and above the central nervous mass (Figure 1.5) while the two coecae are located laterally of the body (not shown). The ventriculus is connected anterioventrally with the oesophagus and posteriodorsally with the excretory organ. Two coecae extend from the ventriculus posteriolaterally and occupy most of the lateral body cavity. The 2 coecae are separated by the excretory organ. The midgut wall is provided with a muscular layer which is responsible for peristalsis, while contractions of the dorsoventral muscles may contribute to mixing of the midgut contents. Usually the content of the midgut is responsible for the color of the live animal. The excretory organ excretes guanine in the form of birefringent spherules, thus performing a function analogous to the malpighian tubules of insects (Helle and Sabelis 1985).

1.8 Aim of this study

Based on previous studies CYP392A16 is overexpressed in resistant strains as well as in susceptible strains after transfer to a more chemically challenging host plant (Dermauw et al. 2013) and it has been shown to metabolize abamectin (Riga et al. 2014). Additionally, CYP392D2, CYP392D8 and CYP392D10 were also found to be overexpressed in multi-resistant strains according to the same study (Dermauw et al. 2013). Moreover, CYP392A11 and CYP392A12 were found to be overexpressed through genome-wide expression data and it was shown that CYP392A11 can metabolize both fenpyroximate and cyenopyrafen (Khaligi et al. 2015, Riga et al. 2015).

Regarding GSTs and their role in resistance development of the two-spotted spider mite, previous studies have indicated the involvement of TuGSTd10 and TuGSTd14. This was based on the analysis of microarray-based transcriptional data in multi-resistant strains, while no additional information regarding the exact role of these two are available to date (Dermauw et al. 2013). Furthermore, TuGSTd05 presented high levels of expression in resistant strains, while *in vitro* metabolism assays showed that TuGSTd05 is capable of metabolizing the METI insecticide cyflumetofen (Pavlidi et al. 2017).

Intradiol-ring cleavage dioxygenases are a newly discovered enzyme family of *T. urticae* and little is known about their function in this organism. Several studies have correlated their function with digestion or detoxification due to the sequence similarity with already known ID-RCDs, while transcriptomic data further support this suggestion (Grbíc et al. 2011, Dermauw et al. 2013, Bryon et al. 2013).

The aim of this study is the immunolocalization of representative enzymes belonging to each family (CYP392, GST, ID-RCD) using specific antibodies and confocal microscopy. The localization of these in a specific tissue could enrich our knowledge regarding the mechanism and physiology underlying insecticide detoxification and resistance in Acari.

2. Materials and Methods

2.1 Tetranychus urticae strains

In this series of experiments we used the spider mite strain Marathonas (Mar-ab) that was collected in 2009, from a highly sprayed rose greenhouse in Marathonas, Athens. The population has been maintained in the lab under abamectin selection (70mg/L) every two generations, on potted kidney bean plants at 25^{o}C, 60% humidity and 16/8h light/dark photoperiod. Additionally, the susceptible spider mite strain London was also used in these series of experiments and it was maintained under the same environmental conditions (temperature, humidity, photoperiod), without acaricide selection.

2.2 Peptide selection for polyclonal antibody production

Protein sequences of *Tetranychus urticae* belonging to three different families of detoxification enzymes [CYP392 subfamilies A, B, C, D, E (CYP392A, CYP392B, CYP392C, CYP392D, CYP392E), GST class delta, omega, mu, kappa, zeta (GSTd, GSTo, GSTmu, GSTk, GSTz), Intradiol Ring-Cleavage Dioxygenases (ID-RCD) (Appendix I)] were downloaded from ORCAE (Online Resource for Community Annotation of Eukaryotes). These sequences were aligned in groups according to their family, using MAFFT v7 (Katoh and Standley 2013). Each multiple alignment was searched manually for a suitable peptide, while conserved motifs, protein domains and 3D structures of the proteins were taken under consideration. Subsequently BLAST (Basic Local Alignment Search Tool) was used to exclude sequence identity with other protein families/subfamilies present in *Tetranychus urticae*. Finally, hydrophobicity tests were conducted (Kyte and Doolittle, 1982) to ensure that the selected peptides do not correspond to transmembrane regions (CYP392) or that they are exposed on the surface of the protein.

The selected peptide sequences were sent to Davids Biotechnologie where additional tools for epitope recognition, hydrophobicity as well as immunogenicity, were used in order to predict and obtain the most suitable antibodies. The peptides that completed the criteria were used for solid-phase peptide synthesis, rabbit immunization and finally affinity purification of the specific antibodies. Each specific antibody was designed to recognize a small number of

proteins from each family that had been previously correlated with acaricide resistance (CYP392A, CYP392D, GSTd) as well as digestion or detoxification (Intradiol Ring-Cleavage Dioxygenase) as described in the first chapter.

2.3 Recombinant protein expression

2.3.1 Intradiol Ring-Cleavage Dioxygenase (Tetur28g01250)

Transformation of *Escherichia coli* Origami (DE3) competent cells was performed with a pET16b vector which encodes tetur28g01250 (28g) from *Tetranychus urticae* His-tagged at the N-terminus. Transformation was followed by bacterial cell culture, single colony selection and inoculation of 3 x 5ml LB, cultured overnight at 37^{o}C/shaking in the presence of ampicillin at a final concentration of 100μg ml^{-1}. An 1/25 dilution from each pre-culture was used to inoculate 3 x 10ml LB and bacteria were grown at 37^{o}C until the culture density reached an OD_{600} of approximately 0.6-0.7. Subsequently, the expression of His_{10}-28g was induced at 37^{o}C using 0.5mM isopropyl β-D-1 thiogalactopyranoside (IPTG). Non-induced (NI) and induced (I) samples were collected and run on a 15% sodium dodecyl sulfate-polyacrylamide gel electrophoresis (SDS-PAGE). Glycerol stocks were made from each pre-culture using a final glycerol concentration of 20%. One of the three pre-cultures was selected to continue the experiment and proceed with large scale culture and production of His_{10}-28g. Bacterial cells were harvested through centrifugation at 4.000rpm for 20min at 4^{o}C. Supernatant was discarded and the bacterial paste was re-suspended in 50ml lysis buffer (500mM NaCl, 50mM Tris-HCl pH=8, 0.2mM EDTA, 10% glycerol) to which 1mM of phenylmethylsulfonylfluoride (PMSF) was added. The re-suspended bacterial paste was sonicated (50 x 30sec sonication – 50 x 30sec on ice) in order for the cell membranes to be agitated and eventually disrupted. Sonication was followed by centrifugation at 12.000rpm for 40min at 4^{o}C in order to collect the supernatant and remove cell debris. Supernatant and pellet samples were collected and run on a 15% SDS-PAGE. Bradford assay (Bradford 1976) was conducted to the supernatant using BSA (Bovine Serum Albumin) as a standard in order to estimate the total protein concentration. The supernatant was kept in aliquots at -20^{o}C until further use in Western blot analyses as positive control.

2.3.2 Glutathion S-Transferase class delta 5, TuGSTd05 (Tetur01g02510)

Glycerol stock of *Escherichia coli* BL21 (DE3) competent cells, that have been previously transformed with a pET100/D-TOPO vector, which contains the coding sequence of glutathione S-transferase class delta 5 of *Tetranychus urticae* (TuGSTd05), was streaked in LB-agar plates. A single colony was used to inoculate 1 x 5ml LB, 100μg ml^{-1} ampicillin and the pre-culture was incubated overnight at 37^{o}C. Two hundred μl of the pre-culture were used to inoculate 10ml LB, 100μg ml^{-1} ampicillin and the cells were allowed to proliferate at 37^{o}C until the culture density reached an OD_{600} of >0.7. The expression of TuGSTd05, His-tagged at the N-terminus, was induced by the addition of 1mM IPTG and further incubation at 37^{o}C. Non-induced (NI) and induced (I) samples were collected from the culture and run on a 15% SDS-PAGE to visualize the achieved expression levels and the experiments were continued. After streaking on LB-agar plates from the glycerol stock, a single colony was selected to inoculate 50ml LB, 100μg ml^{-1} ampicillin and it was left overnight at 37^{o}C. Twenty ml from the pre-culture were used to inoculate 1lt LB (x2) and when the OD_{600} of the culture reached ~0.7, induction of the expression of His_6-TuGSTd05 was conducted by the addition of 1mM IPTG for 4h at 37^{o}C. The induction was followed by centrifugation of the total culture (2lt) at 4.000rpm for 20min at 4^{o}C in order to discard the LB and keep the bacterial paste. The bacterial paste was flash-frozen and stored at -80^{o}C until purification.

2.4 Recombinant protein purification

2.4.1 Glutathion S-Transferase class delta 5, TuGSTd05 (Tetur01g02510)

The purification protocol was based on Pavlidi et al. 2017 with some modifications. The cell pellet was thawed on ice and resuspended in 25ml of lysis buffer (20mM phosphate buffer pH=7.4, 500mM NaCl, 40mM imidazole). In order for the cells to be lysed, lysozyme was added at a final concentration of 10μg ml^{-1} and incubated at 4^{o}C for 30min. The incubation was followed by sonication (25 x 30sec sonication, 25 x 30sec on ice) which caused the mechanical agitation of bacterial membranes and finally their disruption. Cell lysate was centrifuged at 12.000rpm for 30min at 4^{o}C in order to separate the clear lysate from cell debris. Before moving on to the purification, a sample was taken from the supernatant (sn) and the pellet (p), after its resuspension in 1/3 of the initial lysis buffer volume. These samples were run on a 15% SDS-

PAGE to confirm expression and presence of His_6-TuGSTd05 in the soluble part of the cell (sn). The supernatant was loaded in 800μl agarose bed Ni-NTA affinity chromatography column which had been previously equilibrated with 8ml of binding buffer (20mM phosphate buffer pH=7.4, 500mM NaCl, 40mM imidazole). The supernatant was left to flow through the column and a sample was collected (FT) to ensure that the binding of the protein was successful. Twelve ml of wash buffer were applied onto the column (20mM phosphate buffer pH=7.4, 500mM NaCl, 50mM imidazole) in order to discard any unbound molecules and a sample was also collected (W). Finally, 10 elution fractions (0.5ml/fraction) using 5ml of elution buffer (20mM phosphate buffer pH=7.4, 500mM NaCl, 500mM imidazole, 20% glycerol) were applied for the elution of the protein. Samples were collected from each elution fraction and run on a 15% SDS-PAGE along with the controls (NI, I, sn, FT, W) in order to visualize the elution behavior of our protein. The calculation of protein concentration in the eluate was conducted using Bradford assay with BSA as a standard (Bradford 1976). Finally, the elution fractions that presented the higher yield were pooled together and dithiothreitol (DTT) was added at a final concentration of 20mM to prevent the formation of intramolecular or intermolecular disulfide bonds. The purified protein was kept in aliquots at -20^{o}C until further use in Western blot analyses as positive control.

2.5 Western blot analyses

2.5.1 Confirmation of expression of purified proteins using anti-His antibody

For TuGSTd05, increasing concentrations of the purified protein (1μg, 2μg, 5μg, 10μg) were mixed with protein loading buffer at a final concentration of 1X and boiled at 95^{o}C for 5min. Subsequently, samples were loaded on a 15% SDS-PAGE and run at 100V. Proteins were transferred on a polyvinylidene difluoride (PVDF) membrane, at 350mA using a pre-stained protein marker as a control for transfer. Blocking of the membrane was conducted using 5% non fat dried milk for 1h at room temperature with shaking. The membrane was incubated with the primary antibody (mouse anti-His, 1:500 dilution in 3% milk/1X TBST) overnight at 4^{o}C. Three x 10min washes with 1X TBST were performed in order to remove any unbound antibody molecules and the secondary antibody was incubated on the membrane for 1h at room temperature. The secondary antibody (conjugated with horseradish peroxidase) was mouse

specific and it was used in 1:5000 dilution in 1% milk/1X TBST. Again, 3 x 10min washes with 1X TBST were performed and the signal was captured on a medical X-ray film using enhanced chemiluminescence (ECL). For dioxygenase, the total protein concentration of the sonication supernatant was calculated by Bradford assay and a total of 250μg and 500μg were loaded on a 15% SDS-PAGE. The downstream procedure and antibody dilutions were as previously described.

2.5.2 Test of specific antibodies (anti-CYP392A, anti-CYP392D, anti-GSTd, anti-Dioxygenase)

For each experiment 300 adult females were collected directly from the Mar-ab strain and homogenized in 50ul of protein extraction buffer. The protein extraction buffer was modified

Table 2.1: Quantities of positive controls used in Western blot analyses. The quantities were experimentally determined. CYP392 protein controls (CYP392A12, D2, D8, D10) were not functionally expressed thus it was impossible to calculate the exact P450 concetration. Quantities of total protein content were also used for His_{10}-28g (sonication supernatant). For His_6-TuGSTd05 purified protein was used.

Proteins used as positive controls	Quantity of total protein content (μg)	Quantity of specific protein (ng)
CYP392A11	0.5, 2	6ng
CYP392A12	0.5, 2	unknown
CYP392A16	0.5, 2	14ng
CYP392D2	10	unknown
CYP392D8	10	unknown
CYP392D10	5	unknown
His_{10}-28g	250, 500	unknown
His_6-TuGSTd05	1, 2, 5, 10	1, 2, 5, 10 (μg)

According to the specific experiment (for CYP392 protein family the protein extraction buffer contained 50mM Tris-HCl pH=7.5, 150mM NaCl, 1% Triton X-100, 0.1%SDS, 0.2mM PMSF, 0.5mM EDTA and 1mM protease inhibitor cocktail while for GST and ID-RCD the extraction buffer contained 100mM Tris-HCl pH=7.5, 0.5mM EDTA, 0.2mM PMSF and 1mM protease inhibitor cocktail). After the homogenization of the samples, they were centrifuged at 1.000g for

20min at 4°C and the supernatant was collected. In order to calculate the total protein concentration in the supernatant, Bradford assay was conducted using BSA as a standard. The selected quantities of the homogenate (50μg and 100μg) were mixed with protein loading buffer in 1X final concentration. Proteins previously expressed in bacterial membrane preparations in our lab (CYP392A11, A12, A16, D2, D8, D10) were used as positive controls along with His_{10}-28g and His_6-TuGSTd05 expressed in the framework of this project. The quantities of the positive controls that were used were experimentally determined and presented in detail in Table 2.1.

Table 2.2: Dilutions of primary and secondary antibodies along with blocking conditions used in Western blot analyses are presented**.**

Primary antibody			Secondary antibody	
Name	**Dilution**	**Blocking conditions**	**Name**	**Dilution**
anti-CYP392A	1:1000 in 3% milk/1X TBST	5% milk in 1X TBST	anti-rabbit	1:10.000 in 1% milk/1X TBST
anti-CYP392D	1:250 in 3% milk/1X TBST	5% milk in 1X TBST	anti-rabbit	1:10.000 in 1% milk/1X TBST
	1:250 in 3% BSA/1X TBST	8% BSA in 1X TBST	anti-rabbit	1:10.000 in 1% milk/1X TBST
anti-Dioxygenase	1:500 in 3% BSA/1X TBST	5% BSA in 1X TBST	anti-rabbit	1:10.000 in 1% milk/1X TBST
	1:500 in 3% BSA/1X TBST	8% BSA in 1X TBST	anti-rabbit	1:10.000 in 1% milk/1X TBST
anti-GSTd	1:100 in 3% milk/1X TBST	5% milk in 1X TBST	anti-rabbit	1:10.000 in 1% milk/1X TBST
anti-actin	1:250 in 3% milk/1X TBST	5% milk in 1X TBST	anti-rabbit	1:10.000 in 1% milk/1X TBST
anti-His	1:500 in 3% milk/1X TBST	5% milk in 1X TBST	anti-mouse	1:5.000 in 1% milk/1X TBST

Samples (homogenate/positive controls) were boiled at 95°C for 5min after the addition of sample buffer in 1X final concentration and they were loaded on SDS-PAGE (12% for CYP392, 15% for GSTd and ID-RCD). The downstream Western blot analysis was as previously

described. Primary antibodies were incubated overnight at 4^{o}C in dilutions according to the manufacturer's volumetric analyses (titration determined by ELISA) and were as follows: anti-CYP392A in 1:1000, anti-CYP392D in 1:250, anti-GSTd in 1:100 and finally anti-Dioxygenase in 1:500. All primary antibody dilutions were in 3% milk/1X TBST except an additional trial of anti-Dioxygenase antibody and anti-CYP392D antibody which were in 3% BSA/1X TBST. Dilutions of antibodies are presented in Table 2.2, along with blocking conditions for each experiment. The secondary antibody that was used in all experiments was goat anti-rabbit in 1:10.000 dilution in 1% milk/1X TBST. Finally, the signal was captured on a medical X-ray film using enhanced chemiluminescence (ECL). Mouse anti-actin was also used as a loading control.

2.6 Immunofluorescence and Confocal Microscopy

The anti-CYP392A antibody that was designed in the framework of this project was used in immunofluorescence experiments both on *T. urticae* sections as well as in whole mounts of female individuals belonging to the Mar-ab strain. Additionally, anti-CYP392A16 antibody (1:250 dilution), previously designed and tested by Riga (Riga, PhD, 2016) in Western blot analyses and immunolocalization studies was also used in this project as a tool providing extra information regarding the localization of CYP392As.

2.6.1 Sample preparation for cryosections

Individuals were collected directly from the Mar-ab population (100 adult females) and they were placed in an eppendorf containing 1X phosphate-buffered saline (PBS) and the fixative (4% formaldehyde, methanol free). Samples were left for 1h at 4^{o}C on a rotor. Subsequently, the fixative was removed and the samples were incubated overnight in a cryoprotective solution of 30% sucrose in 1X PBS at 4^{o}C. The fixed individuals were immobilized in Optimal Cutting Temperature (OCT) compound and stored at -80^{o}C until use. Longitudinal sections were obtained using the Leica Cryotome CM 1850 (Institute of Molecular Biology and Biotechnology, IMBB) at a thickness of 5μm. Several modifications of this procedure were tested in order to obtain optimal fixation of the samples as well as optimal sectioning quality. These modifications include the number of the individuals (50-200) per sample, the fixation time of the samples (30min-3h) as well as the fixation temperature (4^{O}C, room temperature).

2.6.2 Immunohistochemistry on *T. urticae* sections

Immunohistochemistry of the obtained sections was based on Igham et al. 2014. More specifically, sections were washed with 0.2% Tween20 in 1X PBS (3 x 5min) followed by a single wash step with 0.2% Triton X-100 in 1X PBS for 10min. Blocking of the samples was conducted using 1:100 Fetal Bovine Serum (FBS) in 0.2% Triton X-100/1X PBS for 1h at room temperature. The primary antibody (anti-CYP392A) was added in 1:500 dilution in blocking serum at 4^{o}C overnight. Three washes were performed with 0.2%Triton X-100/1X PBS (3 x 5min) before the addition of the secondary goat anti-rabbit antibody (Alexa Fluor 488) in 1:1000 dilution in blocking serum. Secondary antibody was incubated for 1h at room temperature in the dark. One 5min wash followed with 0.2% Triton X-100/1X PBS and two 5min washes with 0.2% Tween20/1X PBS. Afterwards, RNase A was added in 1:1000 dilution in 0.2% Tween20/1X PBS and incubated at room temperature for 30min. A single 5min wash was performed with 0.2% tween20/1X PBS and the samples were incubated with To-PRO 3-Iodide in 1:1000 dilution in 0.2% Tween20/1X PBS for 5min at room temperature. Finally, the samples were washed 3 x 5min with 0.2% Tween20/1X PBS and prepared for observation on Leica SP8 inverted confocal microscope (Institute of Molecular Biology and Biotechnology, IMBB). As controls, pre-immune serum (in 1:500 dilution) and goat anti-rabbit (Alexa Fluor 488 in 1:1000 dilution) were used to ensure specificity of the primary antibody.

In our effort to optimize the abovementioned procedure for this specific organism and in order to obtain more solid data, we tested various modifications which included unmasking of the antigen through boiling of the slides in 10mM citric acid pH=2.7 for 2min, blocking with Normal Goat Serum (NGS) and change in incubation time with To-PRO (5-20min).

2.6.3 Whole mount immunolocalization

Adult female individuals were collected from the Mar-ab strain (250-300 per sample) for fixation (procedure based on Jonckheere et al. 2016). Fixation of the samples was conducted in a 1:1 mixture of heptan and 1X PBS/0.5% Triton X-100 with the addition of formaldehyde at a final concentration of 4%, for 3h at 4^{o}C on a rotor. After fixation, the lower aqueous phase was discarded and dehydration of the samples was performed with ice-cold methanol (3 x 10min). The samples were then gradually rehydrated in a 3-step procedure (i. 70% methanol/30% 1X

PBS containing 0.2% Triton X-100, ii. 50% methanol/50% 1X PBS-0.2%Triton X-100, iii. 30% methanol/70% 1X PBS-0.2% Triton X-100) of 5min incubation at each step. Further washing of the samples was performed using 1X PBS/0.2% Triton X-100 (3 x 10min) and the samples were sonicated in an ultrasonic cleaning bath for 15min (30sec sonication, 30sec on ice). Blocking was conducted for 2h at room temperature in blocking buffer (5% BSA in 1X PBS/0.2% Triton X-100) and the samples were then incubated with the primary antibody (anti-CYP392A in 1:500 dilution in blocking buffer, anti-CYP392A16 in 1:250 dilution in blocking buffer) at 4^{o}C overnight. Upon removal of the primary antibody, samples were washed with blocking buffer (4 x 20min) and the secondary antibody containing the fluorophore (Alexa Fluor 488) was added (goat anti-rabbit 1:1000) and incubated at room temperature for 2h. Four washes were performed (20min each) with blocking buffer and the samples were incubated with To-PRO 3-Iodide in 1:1000 dilution in 1X PBS/0.2% Triton X-100 for 20min at room temperature. To-PRO was removed, a single wash step was performed with 1X PBS/0.2% Triton X-100 and the samples were transferred on slides. The slides were observed using the Leica SP8 inverted confocal microscope (IMBB) or alternatively Leica SP1 inverted confocal microscope (Department of Biology, University of Crete).

3. Results

3.1 Intradiol Ring-Cleavage Dioxygenases (ID-RCDs)

3.1.1 Peptide selection for polyclonal antibody production

A total of 17 protein sequences that had been identified as ID-RCDs were downloaded from ORCAE (Appendix I) and multiple alignment was performed using MAFFT v7. Five of these have been found to be differentially expressed upon host plant change (from bean to tomato) or in multiresistant strains of *T. urticae* thus playing a role in xenobiotic metabolism (Dermauw et al. 2013). The peptide selection for antibody production was focused on the abovementioned five protein sequences.

Multiple alignment revealed low sequence identity among the members of this family, a fact that made impossible the recognition of all five members by an antibody raised against a single peptide. For this reason we narrowed down our search for a peptide on 3 of these proteins (tetur13g04550, tetur28g01250, tetur01g00490). The selected peptide belonged to tetur13g04550 and its sequence was PDDLERSDITDGQTGVNLD. In Figure 3.1 a small part of the multiple alignment is shown which contains the selected peptide. The selected peptide is indicated by grey color.

Finally, the selected sequence was tested for its hydrophobicity to ensure that this specific region is exposed on the surface of the protein. The hydrophobicity test revealed good water solubility of the peptide. Subsequently, Basic Local Alignment Search Tool (BLAST) was used with the peptide sequence as query against the *T. urticae* database to ensure that it does not exist in other protein families. BLASTp revealed the existence of this peptide only in members of the ID-RCD family. Table 3.1 shows the Tetur IDs of the five ID-RCDs, the selected peptide and its corresponding sequence of each of the five members along with the % identity between them. Finally, the additional predictions performed by Davids Biotechnologie regarding epitope recognition and antigenicity gave acceptable results (Appendix II).

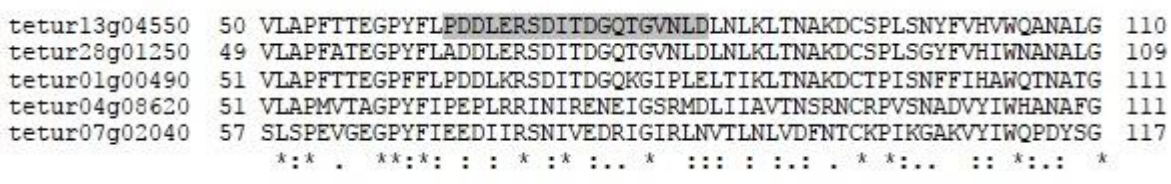

Figure 3.1: Multiple alignment of five members of ID-RCD family. Grey color indicates the selected peptide.

Table 3.1: Tetur ID codes of five members of ID-RCD family, the selected peptide belonging to tetur13g04550 and the corresponding sequences of the rest ID-RCDs, % sequence identity between the selected peptide and the corresponding sequence.

Tetur ID	Selected peptide	% Sequence identity
tetur13g04550	PDDLERSDITDGQTGVNLD (63-82)	
	Corresponding sequences	
tetur28g01250	ADDLERSDITDGQTGVNLD (62-81)	95%
tetur01g00490	PDDLKRSDITDGQKGIPLE (64-83)	74%
tetur04g08620	PEPLRRINIRENEIGSRMD (63-82)	32% *
tetur07g02040	EEDIIRSNIVEDRIGIRLN (70-88)	26% *

*: low % sequence identity could result in no recognition from the antibody

3.1.2 ID-RCD expression

The expression of His_{10}-28g will help us ensure the specificity of the antibody (anti-Dioxygenase). The expressed protein will be used as a positive control in Western blot analyses (95% sequence identity). Several efforts have been made for the expression of His_{10}-28g (MW~29kDa) in 4 different *E. coli* bacterial strains [BL21 (DE3), BL21 (DE3) pLys, JM109 (DE3)] using pET16b and pET26b as cloning vectors. Expression of the protein was visualized on a 15% SDS-PAGE gel by Coomassie Brilliant blue R-250 staining (data not shown). The results showed minimum expression levels and at this point another bacterial strain was tested. Transformation of *E. coli* Origami (DE3) competent cells was performed with pET16b vector containing the sequence of His_{10}-28g (confirmed by sequencing). Induction of expression was followed by the addition of IPTG, while non-induced and induced samples were collected to ensure protein expression (Figure 3.2). In this case, the expression levels of the protein as shown in Figure 3.2 are higher than those previously obtained. Since the reason for this

experiment was to have a positive control and not further downstream analyses of the protein, we obtained the bacterial lysate by sonication and samples were taken from the supernatant (sn) and the pellet (p) after centrifugation to ensure that our protein is in the soluble part of the lysate. Bradford assay was performed to the supernatant, which gave a rough estimate of the total protein concentration that resulted in 25μg μl^{-1}.

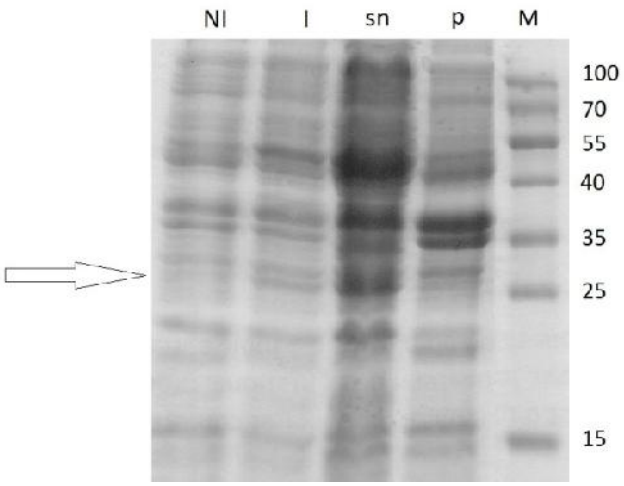

Figure 3.2: SDS-PAGE image showing His_{10}-28g (MW~29kDa) expression indicated by arrow. Non-induced (NI), induced (I), supernatant (sn), pellet (p), protein marker (M).

3.1.3 Confirmation of expression of His_{10}-28g using anti-His antibody

A total amount of 250μg and 500μg from the supernatant were loaded on a 15% SDS-PAGE and after transfer on a PVDF membrane, the membrane was blotted with anti-His antibody in 1:500 dilution in order to confirm the presence of His_{10}-28g. As shown in Figure 3.3, the existence of the recombinant protein was not confirmed by Western blot analysis despite the fact that several alterations of the process were tested (different antibody dilution, BSA/milk for blocking and antibody dilution).

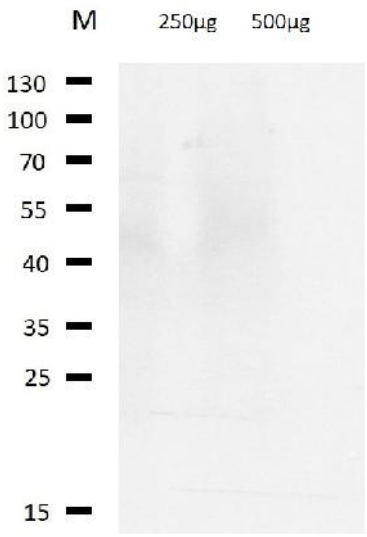

Figure 3.3: Western blot analysis to confirm His_{10}-28g expression. 250µg and 500µg supernatant were loaded. No confirmation of expression. Protein marker (M).

3.1.4 Test of anti-Dioxygenase antibody

The specific antibody against ID-RCD family was tested on the sonication supernatant containing the His_{10}-28g recombinant protein, as well as on population samples after homogenization. Regarding the supernatant, three different conditions were tested and the results are presented in Figure 3.4. As it is shown the antibody presents a slightly altered behavior among the different conditions. The specific antibody seems to recognize a protein at the corresponding molecular weight (~29kDa) at conditions B and C. Additionally the remaining bands are of no importance at this point, since the samples were originated from bacterial cells and not population homogenate. The fact that there are several background bands present indicates that the antibody might not present high specificity for the ID-RCD family.

Population samples were collected and homogenized as described in previous section. 100µg of total protein extract were used to test the specificity of the antibody at two different conditions (those that gave bands at the expected MW when the positive control was used). As Figure 3.5 shows, the antibody presents different recognition pattern between the two experimental conditions. A band is present at the expected molecular weight. The presence of other bands (higher or lower molecular weight proteins) along with the enhanced intensity they present in contrast to the one at the correct MW, indicates that the antibody that was specifically designed to recognize ID-RCD family members, recognizes also other proteins that are present in the organism under study. Additionally, the lack of evidence of dioxygenase expression in the

bacterial supernatant renders it impossible to conclude if the band at the expected MW (~29kDa) corresponds to the desired proteins. The aforementioned reasons make the antibody not suitable for immunolocalization studies.

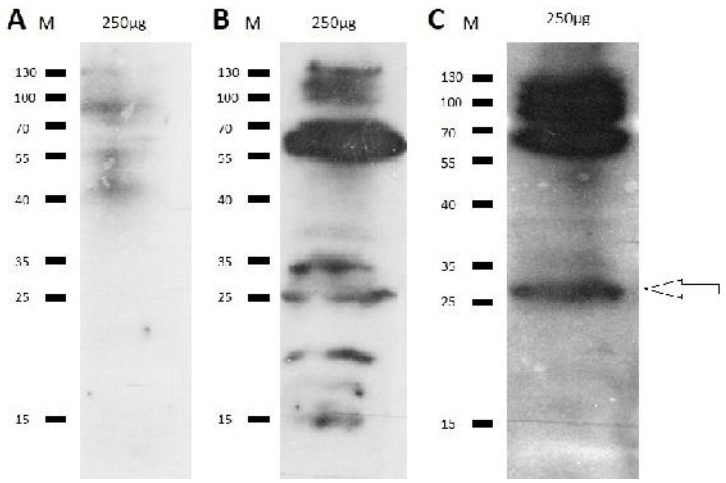

Figure 3.4: Western blot analyses to check the recognition of the positive control (His_{10}-28g) by the specific antibody. 250μg total protein were loaded for each condition. **Condition A:** Overnight blocking with 8% BSA at 4°C, anti-Dioxygenase 1:500 in 3% BSA/1X TBST, incubated at 37°C for 1h. **Condition B:** 1h blocking with 8% BSA at RT, anti-Dioxygenase 1:500 in 3% BSA/1X TBST, incubated overnight at 4°C. **Condition C:** 1h blocking with 5% milk at RT, anti-Dioxygenase 1:500 in 3% milk/1X TBST, incubated overnight at 4°C. Possible recognition of His_{10}-28g is indicated by arrow.

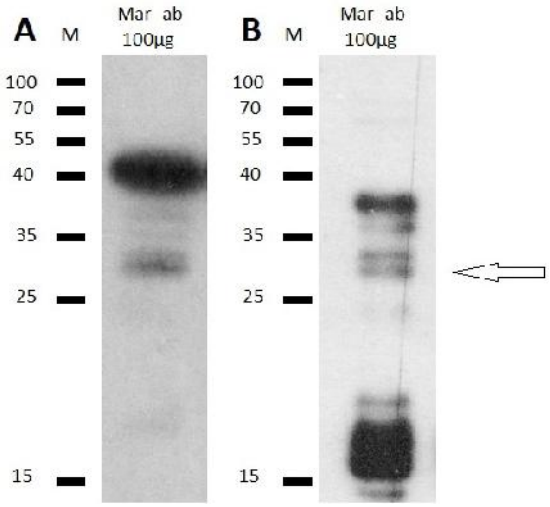

Figure 3.5: Western blot analyses to check specificity of the antibody on population samples. 100μg total protein extract from Mar-ab population were loaded to test each condition. **Condition A:** 1h blocking with 5% milk at RT, anti-Dioxygenase 1:500 in 3% milk/1X TBST, incubated at 4°C overnight. **Condition B:** 1h blocking with 8% BSA, anti-Dioxygenase 1:500 in 3% BSA/1X TBST incubated at 4°C overnight.

3.2 Glutathione S-Transferase (GST) class delta

3.2.1 Peptide selection for polyclonal antibody production

Sixteen protein sequences that belonged to Glutathione S-Transferase family and more specifically class delta GSTs, were downloaded from ORCAE (Appendix I). Multiple alignment was performed using MAFFT v7. Our main goal regarding TuGSTds was to design an antibody that will recognize only TuGSTd05 that has been previously found to directly metabolize cyflumetofen *in vitro* (Pavlidi et al. 2017).

Sequence identity among the proteins of class delta GSTs was high, so it proved impossible to select a peptide for antibody production that will recognize only TuGSTd05. For this reason, we chose a peptide from TuGSTd05 that will possibly recognize other members of delta class GSTs such as TuGSTd14, which also has been shown to be overexpressed in resistant strains (Dermauw et al. 2013). The selected peptide was tested for its hydrophobicity and the results showed medium water solubility. Two additional tests were performed by Davids Biotechnologie that regarded the immunogenicity of the peptide as well as the epitope prediction. Both tests gave satisfactory results (Appendix II).

Subsequently the peptide was aligned with members of GST family, class m, z, o and k, to ensure that the antibody will not recognize any member of these classes. The sequence of the selected peptide is PKDLQARATVDRWLYWDNGSLYASLGAY. Figure 3.6 shows a part of the multiple alignment with the selected peptide in grey color. In Table 3.2 the Tetur IDs are shown, the selected peptide and the corresponding sequence of each protein member along with the % sequence identity between each sequence and the peptide. Finally, BLASTp was used with the peptide sequence as query against the whole protein database of *T. urticae* to ensure specificity of the antibody. The results of BLASTp contained only members of GST family and more specifically class delta GSTs.

```
tetur01g02230   61 GFALWESRAIMTYLVNKYAPESSLYPKDVKARATVERWLYWDTGSLYATLFSYYFPII-Q 120
tetur01g02510   61 GFALWESRAIMTYLVNKYAPESSLYPKDLQARATVDRWLYWDNGSLYASLGAYYFPIVRQ 121
tetur01g02480   61 GFALWESRAIMTYLVNKYAPESSLYPKDVKARATVERWLYWDNGSLYPPLVAYYSPIVRY 121
tetur29g00220   63 GFGLWESRAIMTYLINKYEPESSLYPKDIKARATVDRWLYWDTGSLYSTLYFYYTPIVRQ 123
tetur01g02470   61 GFALWESRAIMTYLVNKYAPESSLYPKDVKARATVDRWLYWDAGSLYASIFSYYCPIVWQ 121
tetur26g01450   61 GYALWESRSIITYLVDKFAPGHSLYPTDLQKRATVNRWLYWDSGTFYASLNAYFGPVF-A 120
                   *:.*****:*:***::*: *  ****.*:: ****:****** *::*..:  *: *:.
```

Figure 3.6: Multiple alignment containing the top 6 hits against the selected peptide for TuGSTd05. Peptide is indicated by grey color. tetur01g02230 (TuGSTd01), tetur01g02510 (TuGSTd05),

tetur01g02480 (TuGSTd03), tetur29g00220 (TuGSTd14), tetur01g02470 (TuGSTd02), tetur26g01450 (TuGSTd07).

Table 3.2: Top 6 hits of BLASTp using TuGSTd05 peptide as query. Tetur IDs are also presented. The selected peptide for polyclonal antibody production, the corresponding sequence belonging to each of the 5 proteins along with % sequence identity between them is presented.

Tetur ID	Selected peptide	% Sequence identity
tetur01g02510 (TuGSTd05)	PKDLQARATVDRWLYWDNGSLYASLGAY	
	Corresponding sequences	
tetur01g02480 (TuGSTd03)	PKDVKARATVERWLYWDNGSLYPPLVAY	79%
tetur01g02470 (TuGSTd02)	PKDVKARATVDRWLYWDAGSLYASIFSY	79%
tetur26g01450 (TuGSTd07)	PTDLQKRATVNRWLYWDSGTFYASLNAY	75%
tetur01g02230 (TuGSTd01)	PKDVKARATVERWLYWDTGSLYATLFSY	75%
tetur29g00220 (TuGSTd14)	PKDIKARATVDRWLYWDTGSLYSTLYFY	75%

3.2.2 TuGSTd05 expression and purification

A preliminary experiment was conducted using a glycerol stock of BL21 (DE3) *E.coli* competent cells containing His_6-TuGSTd05 (~25KDa) in a pET100/D-TOPO vector in order to visualize the expression levels and continue with a large scale culture and production of the protein. Samples from non-induced (NI) and induced (I) bacterial cultures were taken and run on a 15% SDS-PAGE. As Figure 3.7 shows, the glycerol stock presented adequate expression levels so we continued with the downstream procedure.

During the purification process His_6-TuGSTd05 was detected in the bacterial supernatant (sn) with minimum presence in the bacterial pellet (p). The recombinant protein was eluted in the first elution fraction and until the ninth. A small amount of His_6-TuGSTd05 was also detected in flowthrough (FT) and wash fractions, which could be appointed to high imidazole concentration in the lysis buffer and the wash buffer. Figure 3.7 shows the elution behavior of His_6-TuGSTd05.

Since the purpose of this experiment is not further biochemical analysis of TuGSTd05, the elution fractions were pooled together. Bradford assay gave a rough estimation of the concentration of the protein which was calculated at 17.5μg μl^{-1}. Dilutions were made to a final

concentration of 2μg μl^{-1} and 20mM of DTT were added in order to avoid aggregations. Protein was stored at -20^{O}C until further use.

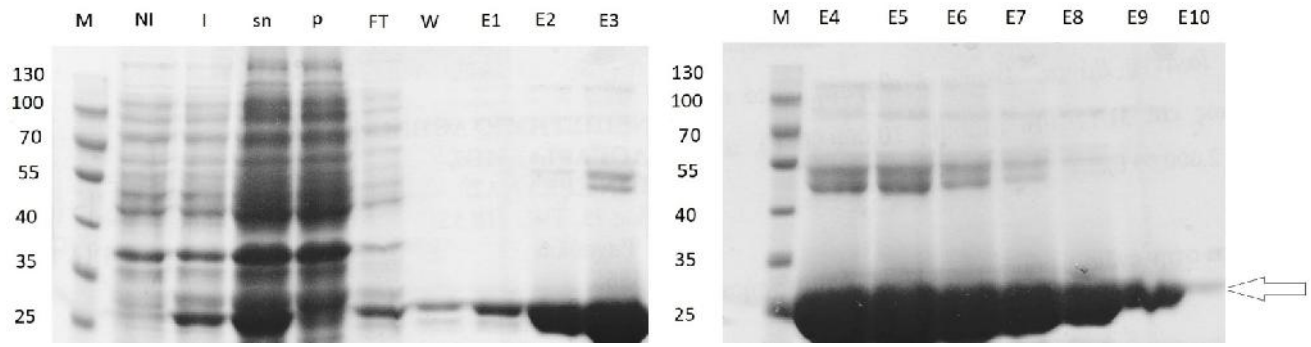

Figure 3.7: SDS-PAGE gel showing the concentration of His_6-TuGSTd05 qualitatively in supernatant (sn), pellet (p), flowthrough (FT), wash (W) and elution fractions (E1-E10). Marker (M), non-induced (NI), induced (I).

3.2.3 Confirmation of expression of His_6-TuGSTd05 using anti-His antibody

A total amount of 1μg, 2μg, 5μg and 10μg of the purified protein were loaded on a 15% SDS-PAGE. Subsequently proteins were transferred on a PVDF membrane and membrane was immunoblotted using anti-His antibody in 1:500 dilution. As Figure 3.8 shows, the expression of the protein was confirmed.

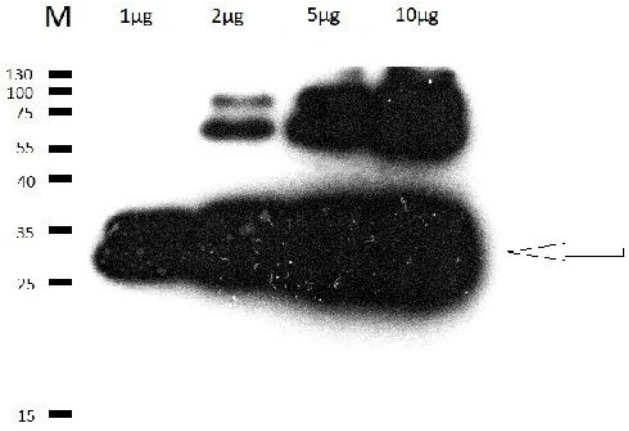

Figure 3.8: Western blot analysis of His_6-TuGSTd05 (~25KDa) with anti-His antibody in 1:500 dilution in 3% milk/1X TBST. The expression of the recombinant protein is confirmed. Higher molecular weight bands could correspond to His_6-TuGSTd05 aggregates.

3.2.4 Test of anti-TuGSTd antibody

The antibody that was designed to recognize specifically a few members of the GST family class delta was tested on the purified protein. Several quantities of the purified protein were used to verify the specificity of the antibody (1μg, 2μg, 5μg, 10μg). The anti-TuGSTd05 antibody was used in 1:100 dilution since higher dilutions did not give any signal. Despite the high antibody concentration, the great amount of the positive control that was loaded and high exposure time of the film, no signal was detected (Figure 3.9A). Ponceau-S staining of the membrane followed in order to confirm the presence of the protein. As Figure 3.9B shows, a band is present at the corresponding MW.

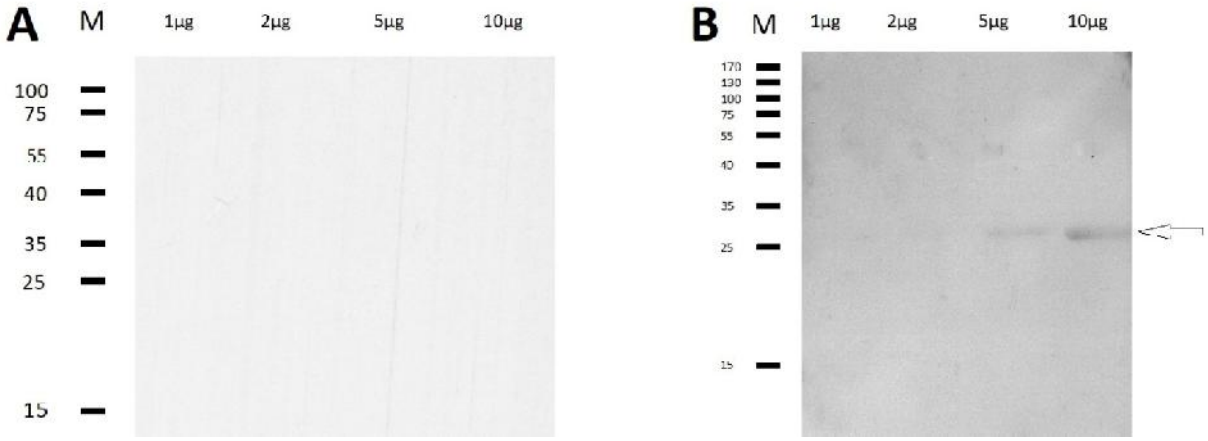

Figure 3.9: A. Western blot analysis of anti-TuGSTd05 antibody using the positive control (His_6-TuGSTd05 in 1μg, 2μg, 5μg, 10μg). Antibody dilution: 1:100 3% milk/1X TBST. **B.** Membranes used in aforementioned Western blot, stained with Ponceau-S. Arrow indicates the purified protein.

3.3 Cytochrome P450 family 392 (CYP392)

A total of 27 protein sequences (18 CYP392 subfamily A, 8 CYP392 subfamily D plus CYP392D10a) were downloaded from ORCAE (Appendix I) and multiple alignment was performed. In this case we aimed in designing two antibodies that would be able to discriminate the two subfamilies (CYP392A, CYP392D). Members of the same family share more than 40% identity at the amino acid level and members of the same subfamily more than 55%. For this reason we focused our search for a suitable peptide in the most differentiated region of the protein sequences (200-325a.a.) as is shown in Figure 3.10. Sequence motifs, as described in Chapter 1 of this work, were annotated and avoided during the peptide selection process. Each selected peptide was aligned with the members of the other subfamily to infer if the % sequence

identity could result in subsequent recognition from the antibody. As Figure 3.11 presents, the identities are few, so possible cross-recognition is minimized. The sequences of the two selected peptides were KCFQIVDSHIQDEIDKHQEK for CYP392A and KVTSNQKELEEKITVEVIKHKEKKATHE for CYP392D. Peptides were tested for their hydrophobicity and the results gave medium water solubility of the CYP392A peptide and good water solubility for the CYP392D (Appendix II). Finally, each peptide was used as a query in BLASTp and the results contained only members of the same subfamily. Table 3.3 shows the Tetur IDs of six CYP392 family members (3 CYP392A, 3 CYP392D), the selected peptide for polyclonal antibody production (indicated also in grey in Figure 3.10), the corresponding peptides and the % sequence identity between them.

```
tetur03g00830  180 IVNNVSILLFGHKYDL--NDPAAIEISAANDEIASSLNFAGVMAFLPWLSSFVFKFKFIN 237
tetur03g00970  180 IVNNISILLFGHKYDH--DDPAAIAISAANEEIGSSLNFAGVMAFLPWLTTIVFKFKLFN 237
tetur06g04520  180 VTNNVSILLFGHKYER--DDPTAIAISSANTEVGRSFSFAGVVAFLPWLAELVFKFELFN 237
tetur03g04990  179 VANNISILMFGHRFEY--NDPFGIELRHNMKQVSDNVDYFTKFIFTTSLSFLIPLAAHFS 238
tetur03g05070  179 VANNISILMFGHRFEY--DDPIGNEMRRNMQKVSDNIEYFTKFVFMPAIFFFVSLAAKFS 238
CYP392D10a     179 VANNISILLFGHGFEYTGTDPIASEMCRNMRQVINNIEYFSKFMFMPSIKFFVFLAAQFN 238
                   :.**:***:*** ::    ** .  :     ::  ...:   . * . :  ::     :.

tetur03g00830  238 --LTRLIKCFQIVDTHIQNEIDKHQEKN-SQEVVDYIDGYLAEMKKREERNQIDDNFSIE 295
tetur03g00970  238 --LAKVLKCFQIVDSHIQDEIDKHQEKN-SQEVVDYIDGYLAEMKRREKQTKVDDNFSID 295
tetur06g04520  238 --VTRLKKCFQIVDTHIQDEIVKHQEKN-SQEVVDYIDGYLVEKKNREKQNKVDDNFTIE 295
tetur03g04990  239 SDHEKVTSNQKDLEDKVTIEVAKHREKQTTHEIEDYIDGFLQEM---DKQKDSNTSFNIN 296
tetur03g05070  239 PELRNANSSQKELEEKITEEVTKHREKKATHEIEDYIDGYLQEM---DKLKDSNLSFDMN 296
CYP392D10a     239 SELKKVTSNQKELEEKITVEVIKHKEKKATHEIEDYIDGYLQEM---DKQKDSNTSFNMD 296
                      .  .  : :: ::  *: **:**: ::*: *****:* *    :: .. : .* ::

tetur03g00830  296 ILKKNAGAFYGAGTAAVSSTMEWMMVYLVRYPEIQDKIRSEIADVIGFERRPDYVDRIRM 356
tetur03g00970  296 ILRRNAASFYGAGTETVASTMEWVMIYLVKYPEYQDKIRSEIADVIGFERRPDFVDRNRM 356
tetur06g04520  296 ILRRNAGAFYGAGTETVSSTMEWIMVYLVKYPEYQDKIRSEIADVIGFERKPDYVDRNRM 356
tetur03g04990  297 TLRRNAADFYAAGSDTTTHVLNFMMLYLVTYPEHQQKIRDEIKQTIGFDRQPDYADRASM 357
tetur03g05070  297 TLRRNTADFYAAGSDTTTNTLSFMMLYLITYPEYQQKIRDEIKETIGFERQPDYADRTSM 357
CYP392D10a     297 TLRRNTADFYAAGADTTTLVLNHMMLYLITYPEYQQKIREEIKQTIGFERQPDYEDRTSM 357
                    *::*:. **.**: :.: .:. :*:**: *** *:***.** :.***:*:**: **  *
```

Figure 3.10: Part of multiple alignment showing the most differentiated region between CYP392A and CYP392D [CYP392A: tetur03g00830 (CYP392A12), tetur03g00970 (CYP392A11), tetur06g04520 (CYP392A16), CYP392D: tetur03g04990 (CYP392D2), tetur03g05070 (CYP392D8), CYP392D10a-obtained by sequencing of the corresponding gene]. Grey color indicates the selected peptides.

Figure 3.11: A. Part of alignment of three representatives of CYP392A subfamily [CYP392A12 (tetur03g00830), CYP392A11 (tetur03g00970), CYP392A16 (tetur06g04520)] against the selected peptide for CYP392D subfamily. **B.** Part of alignment of three representatives of CYP392B subfamily [CYP392D2 (tetur03g04990), CYP392D8 (tetur03g05070), CYP392D10a] against the selected peptide for CYP392A subfamily. Low identity is presented and minimum recognition from the antibody is expected.

Table 3.3: Tetur IDs of selected members of both CYP392 subfamilies are provided. The selected peptide for each subfamily is indicated, the corresponding peptides of the remaining proteins and the % sequence identity between them are also presented.

CYP392 Subfamily A		
Tetur ID	**Selected peptide**	**% Sequence Identity**
tetur03g00970 (CYP392A11)	KCFQIVDSHIQDEIDKHQEK	
	Corresponding sequence	
tetur03g00830 (CYP392A12)	KCFQIVDTHIQNEIDKHQEK	90%
tetur06g04520 (CYP392A16)	KCFQIVDTHIQDEIVKHQEK	90%
CYP392 Subfamily D		
Tetur ID	**Selected peptide**	**% Sequence Identity**
CYP392D10a	KVTSNQKELEEKITVEVIKHKEKKATHE	
	Corresponding sequence	
tetur03g05070 (CYP392D8)	NANSSQKELEEKITEEVTKHREKKATHE	84%
tetur03g04990 (CYP392D2)	KVTSNQKDLEDKVTIEVAKHREKQTTHE	72%

3.3.1 Test of anti-CYP392A antibody

In this experiment we used as positive controls CYP392A11, A12 and A16 that have been previously expressed in bacterial membranes from members of our lab (Tsakireli, Riga). A11 and A16 were functionally expressed, so a peak at 450nm could be detected and the exact concentration of them was calculated. A12 was not functionally expressed thus only the total protein concentration was known. Six ng of A11, 2μg total protein of A12 and 14ng of A16 were loaded on a 12% SDS-PAGE. After their transfer on a PVDF membrane, anti-CYP392A was used for immunoblotting in 1:1000 dilution. The result gave a clear recognition image since there is no background and the band that is present corresponds to the correct molecular weight of the proteins (~57kDa) (Figure 3.12). Additionally, when this result is interpreted along with the bioinformatics analyses, we can conclude that these two are in accordance. The antibody appears to have higher specificity for A11, which was the source of the peptide (antigen) and lower specificity for A16 with which the peptide had 74% identity.

The antibody was subsequently tested on population samples belonging to both the resistant (Mar-ab) and the susceptible strain (London). Fifty and 100μg of each homogenate were used for Western blot analysis with 1:1000 anti-CYP392A. The result gave one band at the expected molecular weight (slightly lower than the controls, a characteristic behavior previously

observed by Riga, PhD) with no background (Figure 3.12). This indicates that the anti-CYP392A antibody could be used for immunoloclization studies. Anti-actin was used for loading control in 1:500 dilution but the antibody gave a multiple-band pattern, so it can not be used as loading control.

Finally, the anti-CYP392A was tested on CYP392D controls (D2, D8, D10) to ensure that recognition of subfamily D has been avoided. 10μg total protein from control/bacterial membranes were loaded on a 12% SDS-PAGE and after their transfer on a PVDF membrane anti-CYP392A was used in 1:1000 dilution. Western blot analysis did not give any signal under these conditions thus we can assume that anti-CYP392A does not recognize members of D subfamily (data not shown).

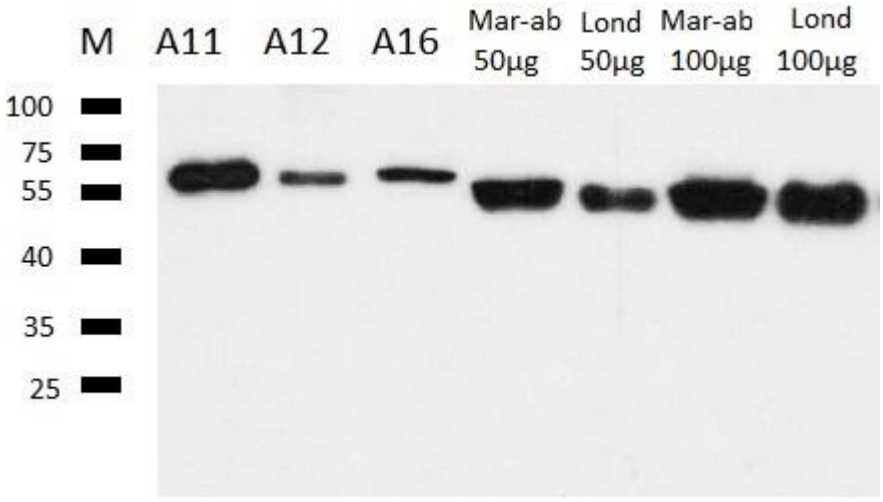

Figure 3.12: Western blot analysis of anti-CYP392A (1:1.000) against positive controls and populations. CYP392A11 (tetur03g00970): 6ng, CYP392A12 (tetur03g00830): 2μg total protein, CYP392A16 (tetur06g04520): 14ng. The intensity of the bands shows high specificity of the antibody for CYP392A11 and low for CYP392A16. A band is present at the correct MW in the population samples.

3.3.2 Test of anti-CYP392D antibody

The positive controls used in this experiment were CYP392D2, D8 and D10. All of them have been previously expressed in bacterial membranes (Tsakireli, Riga) but not functionally. The exact P450 content of the preparations could not be calculated and for this reason samples were loaded according to the total protein concentration and they were adjusted experimentally. A total of 5μg of D10 and 10μg of D2 and D8 were loaded on a 12% SDS-PAGE and after they were transferred on a PVDF membrane, anti-CYP392D was used for immunoblotting in 1:250

dilution. The result is shown in Figure 3.13 were a band is present at the correct molecular weight.

Furthermore, anti-CYP392D was tested on population samples (Mar-ab). 50μg and 100μg of population homogenate were loaded on a 12% SDS-PAGE and upon their transfer on a PVDF membrane, anti-CYP392D was used for immunoblotting in 1:250 dilution. Figure 3.13 shows that there is no band at the expected molecular weight regarding the population samples (it becomes visible after higher exposure times, data not shown). To eliminate any doubts considering the specificity of the antibody we also tested it in different experimental conditions (Figure 3.14). The additional bands were not only present but they gained in intensity. Additionally, a band at the correct MW became visible (D10 was used as positive control). Despite this, as it is indicated by the results, the anti-CYP392D is not specific for the members of CYP392 subfamily D and it can not be used in immunolocalization studies.

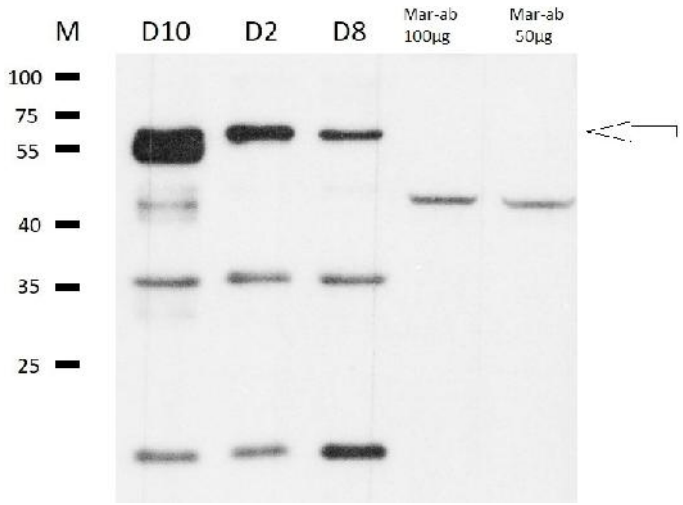

Figure 3.13: Western blot analysis using anti-CYP392D against controls and populations. Anti-CYP392D dilution 1:250 3% milk/1X TBST. CYP392D10: 5μg total protein, CYP392D2 (tetur03g04990): 10μg total protein, CYP392D8 (tetur03g05070):10μg total protein.

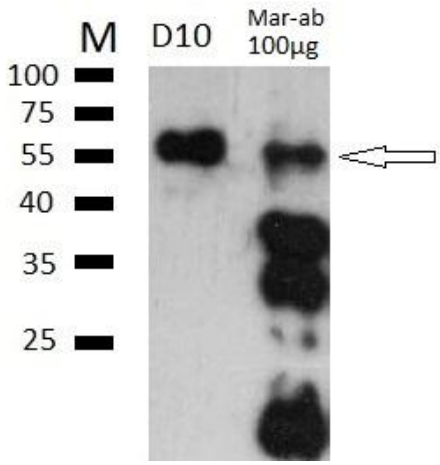

Figure 3.14: Western blot analysis using anti-CYP392D (alternative conditions) 1:250 3% BSA/1X TBST. CYP392D10: 5µg, Mar-ab: 100µg.

3.4 Immunolocalization of CYP392A subfamily and CYP392A16

A series of immunolocalization experiments was conducted either on cryo-sections or on whole mount tissue specimens both derived from adult *T. urticae* females. Our efforts were focused mainly in finalizing the immunolocalization protocol using the anti-CYP392A16 and anti-CYP392A antibody in order to obtain consistent data.

Anti-CYP392A16 was used in 1:250 dilution on both sections and whole mount specimens, while anti-CYP392A was used in 1:500 dilution (mostly sections). Regarding anti-CYP392A16 antibody, in most experiments it resulted in high background and seldom was the signal specific. Here, a part of the data is presented indicating a possible location for CYP392A16. In Figure 3.15 (left), a ventral view of a whole mount female specimen is presented, where A16 is localized near the Central Nervous Mass (CNM). Figure 3.16 shows the gnathostoma of a female spider mite along with the first pair of legs, where a potentially positive signal was often detected. On the other hand, anti-CYP392A antibody gave even more controversial results regardless of the preparation process of the sample (cryo-sections or whole mount) (data not shown).

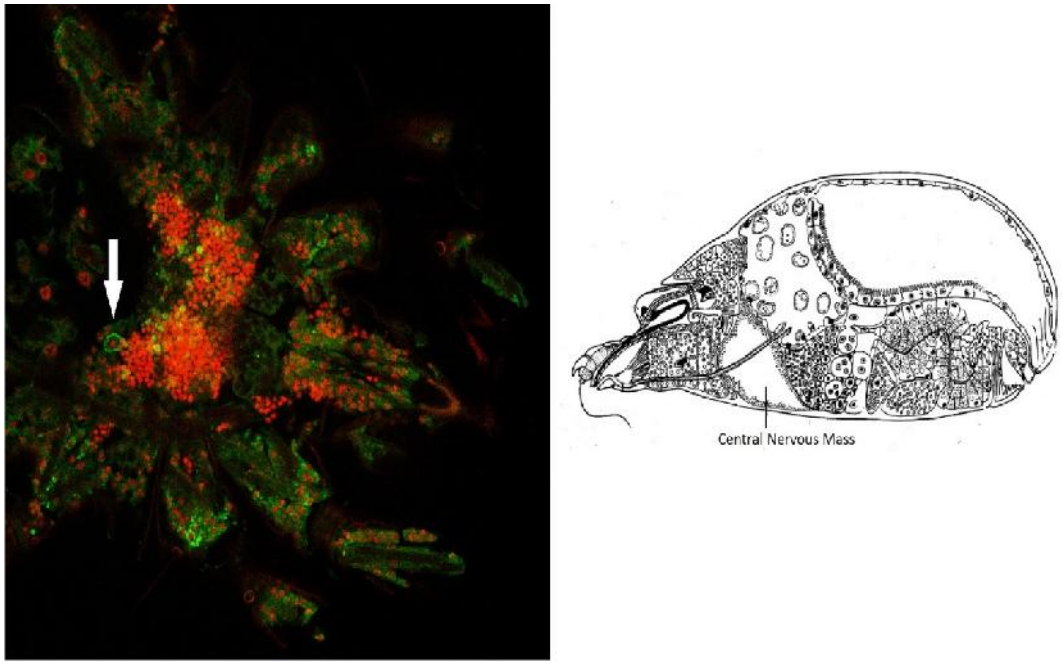

Figure 3.15: Immunolocalization of CYP392A16 using anti-CYP392A16 antibody in 1:250 dilution on whole mount specimens. Ventral view of a female spider mite is shown (left). Green color: anti-CYP392A16, red color: DNA staining with To-PRO (cell nucleus), white arrow: possible specific signal. Image obtained on SP1 inverted confocal microscope. A schematic representation of the internal antomy of the spider mite is also shown (right), indicating the position of Central Nervous Mass (CNM). Image taken by Balabanidou, Riga, Papadaki.

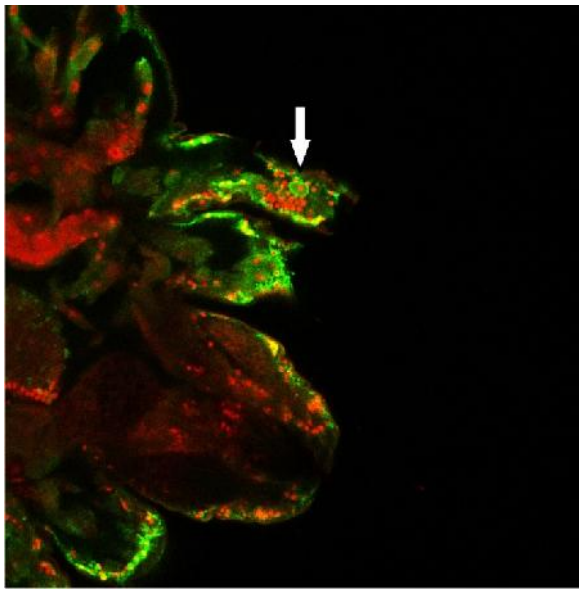

Figure 3.16: Immunolocalization of CYP392A16 using anti-CYP392A16 antibody in 1:250 dilution on whole mount specimens. Gnathostoma of a spider mite is presented along with the first pair of legs (only one shown). Green: anti-CYP392A16, red: DNA staining with To-PRO (cell nucleus), white arrow: possible specific signal. Image taken by Balabanidou, Riga, Papadaki.

4. Discussion and future plans

The main objective of this project was the study of two major enzyme families (CYP392, GST), which have been previously correlated with detoxification of insecticides/acaricides, through their tissue specific localization in the two-spotted spider mite *Tetranychus urticae*. Additionally, we made an effort to localize members of a newly discovered family in *T. urticae* species with an unknown function so far (ID-RCD). In order to achieve this goal, four antibodies were raised (anti-CYP392A, anti-CYP392D, anti-GSTd, anti-Dioxygenase) and two recombinant proteins were expressed (His_{10}-28g, His_6-TuGSTd05), which were subsequently used as controls in Western blots.

Despite our efforts to produce His_{10}-28g (ID-RCD), as described in sections 2.3.1 and 3.1, we were not able to achieve high protein yield. This is in accordance with previously obtained data from members of our lab (Balabanidou, unpublished). The low protein concentration could also explain the fact that we were not able to confirm the presence of His_{10}-28g in Western blot using anti-His antibody. Protein yield could be improved by using a different affinity tag. Usually Maltose-Binding Protein (MBP) is a good alternative. It provides efficient translation initiation while it enhances the solubility of its fusion partner (Kapust and Waugh 1999). Subsequently, the purified protein could be used for rabbit immunization instead of a synthetic peptide. This could increase the chances of obtaining an antibody of high specificity and it could be suitable for immunolocalization studies. Furthermore, metabolism assays on the purified protein would provide us with valuable information regarding the function of the protein while its crystal structure could further enlighten the mechanism.

The abovementioned practice for antibody production was applied in the case of anti-TuGSTd05 antibody. As described in section 3.2.4 anti-TuGSTd05 did not give any signal despite the high antibody titer and the low-diluted working solutions. For this reason another antibody was raised against the purified protein. Western blot analyses revealed that anti-TuGSTd05-2 is a highly specific antibody (experiments continued by Maria Riga, Elena Vorgia), a rather promising result for future immunolocalization experiments.

Anti-CYP392D antibody was also proven to be unsuitable for immunolocalization studies since it was not specific for the members of subfamily D of family 392 (section 3.3.2). Regardless of protocol modifications, the antibody always showed this recognition pattern a fact that could be attributed to the selected peptide sequence.

Anti-CYP392A antibody was proven a highly specific antibody and it was used in immunolocalization studies. The data we obtained using anti-CYP392A were controversial so we tested several protocol alterations such as minimizing the fixation time, while antigen retreaval through boiling in acidic environment was also tested. Since we were unable to produce consistent data, we attempted to finalize the protocol using the anti-CYP392A16 antibody. Our results do not fully support a safe conclusion regarding the localization of either CYP392A or CYP392A16, but a possible location for CYP392A16 was indicated. A16 was detected in cells near the central nervous mass of *T. urticae*. Several other studies conducted in different organisms have located detoxification enzymes, or even P450 enzymes, that confer resistance in the brain or nerve cord [*Aedes aegypti* (Grigoraki et al. 2016), *Bombyx mori* (Xuan et al.2015), *Tribolium castaneum* (Zhu et al. 2010)]. Additionally, based on the internal anatomy of *T. urticae*, it is known that this organism does not have any tissue that specializes in detoxification. Usually, in other arthropod (insect) species this process takes place mainly in the malpighian tubules [*Trichoplusia ni* (Labé et al. 2011), *Aedes aegypti* (Grigoraki et al. 2016), *Anopheles gambiae* (Lycett et al. 2006), *Drosophila melanogaster* (Yang et al. 2007)] which is considered to have excretory and osmoregulatory function. On the contrary, in *T. urticae* the osmoregulatory function is performed by cells positioned in the lateral walls of the hindgut, while according to Bauvelt the hindgut could be responsible for the transportation of food residue as well as for excretion (Bauvelt 1945). Since CYP392A16 was not detected in the hindgut cells, it could be possible that A16 is expressed in nerve cells. Furthermore, a tissue-specific staining aiming the nervous system could be used in order to further support this hypothesis. A tissue-specific staining (nervous system/muscular system) could also provide us with information regarding the localization of A16 in cells positioned in the leg of *Tetranychus urticae*, since there are no information available on the internal anatomy of the leg.

Furthermore, the anti-CYP392A antibody, since it presented high specificity, it could be used as a diagnostics tool for the discrimination between susceptible and resistant populations based on the protein quantity (Nauen et al. 2015, Devonshire et al. 1986).

To conclude, we were not able to locate members of the family 392 subfamily A but we have an indication regarding the possible location of CYP392A16 in nerve cells. Additional experiments should be conducted and an antibody against CPR (Cytochrome P450 Reductase), the redox partner of class II P450s could be used to strengthen this finding.

Appendix I: List of Tetur codes used

CYP392A	CYP392B	TuGSTd	ID-RCD
tetur02g14020	tetur02g06550	tetur01g02230	tetur07g06560
tetur02g14330	tetur20g03200	tetur01g02470	tetur19g02300
tetur02g14400	tetur08g91631	tetur01g02480	tetur06g00450
tetur03g00830	tetur02g06640	tetur01g02500	tetur44g00140
tetur03g00020	tetur20g00290	tetur01g02510	tetur04g00150
tetur03g00970		tetur03g07920	tetur07g02040
tetur03g09941	**CYP392C**	tetur26g01450	tetur01g00490
tetur06g04520	tetur03g03950	tetur26g01460	tetur04g08620
tetur07g06410		tetur26g01490	tetur13g04550
tetur07g06460	**CYP392E**	tetur26g01500	tetur07g05940
tetur07g06480	tetur27g00340	tetur26g01510	tetur07g05930
tetur08g07950	tetur27g00240	tetur26g02801	tetur19g03360
tetur08g08050	tetur03g05540	tetur26g02802	tetur12g04671
tetur11g04390	tetur27g01030	tetur29g00220	tetur28g01250
tetur11g00530	tetur03g05080	tetur31g01330	tetur06g00460
tetur16g03500	tetur27g00330	tetur31g01390	tetur20g01790
tetur16g03790	tetur06g02400		tetur20g01160
tetur47g00090	tetur03g05100	**TuGSTmu**	
	tetur27g00230	tetur03g09230	
CYP392D	tetur27g00350	tetur05g05180	
tetur03g04990	tetur27g01020	tetur05g05190	
tetur03g05000	tetur27g02598	tetur05g05200	
tetur03g05010	tetur27g00220	tetur05g05210	
tetur03g05030	tetur03g05040	tetur05g05220	
tetur03g05070	tetur06g02820	tetur05g05240	
teturg0309961	tetur03g09961	tetur05g05250	
tetur23g00260	tetur03g9951	tetur05g05260	
tetur03g05020		tetur05g05270	
	TuGSTz	tetur05g05290	
	tetur07g02560	tetur05g05300	
	TuGSTk	**TuGSTo**	
	tetur22g02300	tetur12g03900	
		tetur01g02320	

Appendix II: Selected peptides and their scores for solubility, immunogenicity and epitope prediction

	CYP392A
	KCFQIVDSHIQDEIDKHQEK
Solubility	Medium
Immunogenicity	Medium
Epitope prediction	Good

	CYP392D
	KVTSNQKELEEKITVEVIKHKEKKATHE
Solubility	Good
Immunogenicity	Good
Epitope prediction	Medium

	TuGSTd
	PKDLQARATVDRWLYWDNGSLYASLGAY
Solubility	Medium
Immunogenicity	Good
Epitope prediction	Medium

	ID-RCD
	PDDLERSDITDGQTGVNLD
Solubility	Good
Immunogenicity	Medium
Epitope prediction	Good

References

Balabanidou V, Kampouraki A, MacLean M, Blomquist GJ, Tittiger C, Juarez MP, Mijailovski S, Chalepakis G, Anthousi A, Lynd A, Antoine S, Hemingway J, Ranson H, Lycett G, Vontas J. 2016. *Proc Natl Acad Sci USA* 113: 9268-9273

Bautista MAM, Miyata T, Miura K, Tanaka T. 2009. RNA interference-mediated knockdown of a cytochrome P450, *CYP8BG1*, from the diamondback moth, *Plutella xylostella,* reduces larval resistance to permehtrin. *Insect Biochem Mol Biol* 39:38-46

Bensoussan N, Estrella Santamaria M, Zhurov V, Diaz I, Grbić M, Grbić V. 2016. Plant-herbivore interaction: dissection of the cellular pattern of *Tetranychus urticae* feeding on the host plant. *Front Plant Sci* 7:1105-1118

Bradford MM. 1976. A rapid and sensitive method for microgram quantities of protein utilizing the principle of protein-dye binding. *Anal Biochem* 72:248-254

Brattsten LB, Holyoke CW, Leeper JR, Raffa KF. 1986. Insecticide resistance: challenge to pest management and basic research. *Science* 231(4743):1255-1260

Bryon A, Wybouw N, Dermauw W, Tirry Luc, Van Leeuwen T. 2013. Genome wide gene-expression analysis of facultative reproductive diapause in the two-spotted spider mite *Tetranychus urticae*. *BMC Genomics* 14:815-835

Bostanian NJ, Morisson FO. 1973. Morphology and ultrastructure of sense organs in the two-spotted spider mite (Acarina: Tetranychidae). *Ann Entomol Soc Am* 66:379-383

Campbell PM, Newcomb RD, Russell RJ, Oakeshott JG. 1998. Two different amino acid substitutions in the ali-esterase, E3, confer alternative types of organophosphorus insecticide resistance in the sheep blowfly, Lucilia cuprina. *Ins Biochem Molec Biol* 28:139-150

Cao CW, Zhang J, Gao XW, Liang P, Guo HL. 2008. Overexpression of carboxylestrerase gene associated with organophosphorus insecticide resistance in cotton aphids *Aphis gossyppi* (Glover). *Pest Biochem Physiol* 90:175-180

Clark JM, Scott JG, Campos F. 1994. Resistance to avermectins: extent, mechanisms, and management Implications. *Annu Rev Entomol* 40:1-30

Coon MJ, Vaz AD, Bestervelt LL. 1996. Peroxidative reactions of diversozymes. *FASEB J.* 10:428–34

Croft BA, Strickler K. 1983. Natural enemy resistance to pesticides: documentation, characterization, theory and application. In *Pest Resistance to Pesticides*, ed. GP Georghiou, T Saito, pp. 669–702. New York: Plenum

Cui F, Lin Z, Wang HS, Liu SL, Chang HJ, Reeck G, Qiao CL, Raymond M, Kang L. 2011. Two single mutations commonly cause qualitative change of nonspecific carboxylesterases in insects. *Ins Biochem Molec Biol* 41:1-8

Daborn PJ, Yen JL, Bogwitz MR, Goff GL, Feil E, Jeffers S, Tijet N, Perry T, Heckel D, Batterham P, Feyereisen R, Wilson TG, ffrench-Constant RH. 2002. A single P450 allele associated with insecticide resistance in *Drosophila*. *Science* 297:2253-2256

Dang K, Doggett SL, Veera Singham G, Lee CY. 2017. Insecticide resistance and resistance mechanisms in bed bugs, *Cimex* spp. (Hemiptera: Cimicidae). *Paras & Vect* 10:318

Davies TGE, Field LM, Usherwood PNR, Williamson MS. 2007. DDT, pyrethroids and insect sodium channels. *IUBMB Life* 59:151-162

Dekeyser MA. 2005. Acaricide mode of action. *Pest Manag Sci* 61:103-110

Dermauw W, Ilias A, Riga M, Tsagkarakou A, Grbíc M, Tirry L, Van Leeuwen T, Vontas J. 2012. The cys-loop ligand-gated ion channel gene family of *Tetranychus urticae*: implications for acaricide toxicology and a novel mutation associated with abamectin resistance. *Insect Biochem Mol Biol* 42:455-465

Dermauw W, Wybouw N, Rombauts S, Menten B, Vontas J, et al. 2013. A link between host plant adaptation and pesticide resistance in the polyphagous spider mite *Tetranychus urticae*. *PNAS* 110:E113–22

Devonshire AL, Moores GD, Ffrench-Constant RH. 1986. Detection of insecticide resistance by immunological estimation of carboxylesterase activity in Myzus persicae (Sulzer) and cross reaction of the antiserum with Phorodon humuli (Schrank) (Hemiptera: aphididae). *Bull Entamol Res* 76:97:107

Enayati AA, Ranson H, Hemingway J. 2005. Insect glutathione transferases and insecticide resistance. *Insect Mol Biol* 14(1):3–8

Feyereisen R. 1999. Insect P450 enzymes. *Ann Rev Entomol* 44:507-533

Feyereisen R. 2012. Insect CYP Genes and P450 Enzymes. Insect biochemistry and molecular biology, 236-316

Feyereisen R, Dermauw W, Van Leeuwen T. 2015. Genotype to phenotype, the molecular and physiological dimensions of resistance in arthropods. *Pest Biochem Physiol* 121:61-77

Fraulo AB, Liburd OE. 2007. Biological control of twospotted spider mite, *Tetranychus urticae*, with predatory mite, *Neoseiulus californicus*, in strawberries. *Exp Appl Acarol.* 43(2):109-19

García-Marí F, Gonzáles-Zamora JE. 1999. Biological Control of Tetranychus Urticae (Acari: Tetranychidae) With Naturally Occurring Predators in Strawberry Plantings in Valenica, Spain. *Exp Appl Acarol* 23(6):487-495

Ghosh R, Andersen EC, Shapiro JA, Gerke JP, Kruglyak L. 2012. Natural variation in a chloride channel subunit confers avermectin resistance in *C. elegans*. *Science (New York, N.y)* 335(6068):574-578

Gigon V, Camps C, Le Corff J. 2016. Biological control of *Tetranychus urticae* by *Phytoseiulus macropilis* and *Macrolophus pygmaeus* in tomato greenhouses. *Exp Appl Acarol* 68(1):55-70

Gordon HT. 1961. Nutritional factors in insect resistance to chemicals. *Annu. Rev. Entomol.* 6:27–54

Gotoh O. 1992. Substrate recognition sites in cytochrome P450 family 2 (CYP2) protein inferred from comparative analyses of amino acid and coding nucleotide sequences. *J Biol Chem* 267:83-90

Govella NJ, Chaki PP, Killeen GF. 2013. Entomological surveillance of behavioral resilience and resistance in residual malaria vector populations. *Malaria Journal* 12:124-133

Grbić M, Van Leeuwen T, Clark RM, Rombauts S, Rouzé P, Grbić V, … Van de Peer Y. 2011. The genome of *Tetranychus urticae* reveals herbivorous pest adaptations. *Nature 479*(7374):487–492

Grigoraki L, Lagnel J, Kioulos I, Kampouraki A, Morou E, Labbe P, Weill M, Vontas J. 2015. Transcriptome Profiling and Genetic Study Reveal Amplified Carboxylesterase Genes Implicated in Temephos Resistance, in the Asian Tiger Mosquito Aedes albopictus. *PLoS Negl Trop Diseas* 9:e0003771

Grigoraki L, Balabanidou V, Meristoudis C, Miridakis A, Ranson H, Swevers L, Vontas J. 2016. Functional and immunohistochemical characterization of CCEae3a, a carboxylesterase associated with temephos resistance in the major arbovirus vector *Aedes aegypti* and *A. albopictus*. *Insect Biochem Molecul Biol* 74:61-67

Habig WH, Pabst MJ, Jakoby WB. 1974. Glutathione S-transferases. *J Biol Chem* 249: 7130–7139

Haddi K, Berger M, Bielza P, Cifuentes D, Field LM, Gorman K, Rapisarda C, Williamson MS, Bass C. 2012. Identification of mutations associated with pyrethroid resistance in the voltage-gated sodium channel of the tomato leaf miner (*Tuta absoluta*). *Ins Biochem Molec Biol* 42:506-513

Hayashi N, Sasama Y, Takahashi N, Ikemi N. 2013. Cyflumetofen, a novel acaricide - its mode of action and selectivity. *Pest Manag Sci* 69, 1080-1084

Hayes JD, Pulford DJ. 1995. The glutathione S-transferase supergene family – Regulation of GST and the contribution of the isoenzymes to cancer chemoprotection and drug resistance. *Crit Rev Biochem Mol Biol* 30:445–600

Heckel DG. 2012. Ecology. Insecticide resistance after Silent Spring. *Science* 337(6102):1612-1614

He C, Xie W, Yang X, Wang SL, Wu QJ, Zhang YJ. 2018. Identification of glutathione S-transferase in *Bemisia tabaci* (Hemiptera:Aleyrodidae) and evidence that GSTd7 helps explain the difference in insecticide susceptibility between B. tabaci Middle east-Minor Asia 1 and Mediterranean. *Insect Mol Biol* 27:22-35

Helle W, Sabelis MW. 1985. Spider mites: their biology, natural enemies and control. *World Crop Pests* Vol 1A and 1B

Hollingworth R, Ahammadsahib K. 1995. Inhibitors of respiratory complex I: mechanisms, pesticidal actions and toxicology. *Reviews in Pesticide Toxicology* 3: 301-310

Hostetler ME, Brenner RJ. 1994. Behavioral and physiological resistance to insecticides in the German Cockroach (Dictyoptera: Blattellidae): an experimental reevaluation. *J Econom Entomol* 87:885-893

Ingham VA, Jones CM, Pignatelli P, Balabanidou V, Vontas J, Wagstaff SC, Moore JD, Ranson H. 2014. Dissecting the organ specificity of insecticide resistance candidate genes in *Anopheles gambiae*: known and novel candidate genes. *BMC Genomics* 15:1018-1027

Jonckheere W, Dermauw W, Zhurov V, Wybouw N, Van den Bulcke J, Villarroel CA, Greenhalgh R, Grbíc M, Schuurink RC, Turry L, Baggerman G, Clark RM, Kant MR, Vanholme B, Menschaert G, Van Leeuwen T. 2016. The salivary protein repertoire of the polyphagous spider-mite *Tetranychus urticae*: a quest for effectors. *Mol and Cell Proteom* 15:3594-3613

Jones CM, Liyanapathirana M, Agossa FR, Weetman D, Ranson H, Donnelly MJ, Wilding CS. 2012. Footprints of positive selection associated with a mutation (N1575Y) in the voltage-gated sodium channel of Anopheles gambiae. *Proc Nat Acad Sci USA* 109:6614-6619

Juarez MP, Fernandez GC. 2007. Cuticular hydrocarbons of triatomines. *Comp Bioch Physiol* 147:711-730

Kane NS, Hirschberg B, Qian S, Hunt D, Thomas B, Brochu R, Ludmerer SW, Zheng Y, Smith MH, Arena JP, Cohen CJ, Schmatz D, Warmke J, Cully DF. 2000. Drug-resistant *Drosophila* indicate glutamate-gated chloride channels are targets for the antiparasitics nodulisporic acid and ivermectin. *PNAS* 97:13949-13954

Kapust RB, Waugh DS. 1999. Escherichia coli maltose-binding protein is uncommonly effective at promoting the solubility of polypeptides to which it is fused. *Protein Sci* 8:1668-1674

Karunker I, Benting J, Lueke B, Ponge T, Nauen R, Roditakis E, Vontas J, Gorman K, Denholm I, Morin S. 2008. Over-expression of cytochrome P450 *CYP6CM1* is associated with high resistance to imidacloprid in the B and Q biotypes of *Bemisia tabaci* (Hemiptera: Aleyrodidae). *Insect Biochem Mol Biol* 38:634-644

Katoh K, Standley DM. 2013. MAFFT Multiple Sequence Alignment Software version 7: Improvements in Performance and Usability. *Mol Evol Biol* 30(4)772-780

Khajehali J, Van Nieuwenhuyse P, Demaeght P, Tirry L, Van Leeuwen T. 2011. Acaricide resistance and resistance mechanisms in *Tetranychus urticae* population from rose greenhouses in the Netherlands. *Pest Manag Sci* 67(11):1424-1433

Khalighi M, Dermauw W, Wybouw N, Bajda S, Osakabe M, Tirry L, Van Leeuwen T. 2015. Molecular analyses of cyenopyrafen resistance in the two-spotted spider mite*Tetranychus urticae*. *Pest Manag Sci* 72:103-112

Khalighi M, Tirry L, Van Leeuwen T. 2014. Cross-resistance risk of the novel complex II inhibitors cyenopyrafen and cyflumetofen in resistant strains of two-spotted spider mite *Tetranychus urticae*. *Pest Manag Sci* 70:365-368

Knowles CO. 1997. Mechanisms of resistance to acaricides. Sjut, V. (Ed.), Molecular Mechanisms of Resistance to Agrochemicals. Springer, New York, 57-77

Kwon DH, Yoon KS, Clark JM, Lee SH. 2010. A point mutation in a glutamate-gated chloride channel confers abamectin resistance in the two-spotted spider mite *Tetranychus urticae* Koch. *Insect Mol Biol* 19:583-591

Kyte J, Doolittle RF. 1982. A simple method for displaying the hydropathic character of a protein. *J Mol Biol* 157(1):105—132

Labbé R, Caveney S, Donly C. 2011. Expression of multidrug resistance proteins is localized principally to the Malpighian tubules in larvae of the cabbage looper moth, *Trichoplusia ni*. *J Exper Biol* 214:937-944

Lockwood JA, Byford RL, Story RN, Sparks TC, Quisenberry SS. 1985. Behavioral resistance to pyrethroidsin the horn fly *Haematobia irritans* (Diptera:Muscidae). *Envir Entomol* 14:873-880

Lycett GJ, McLaughlin LA, Ranson H, Hemingway J, Kafatos FC, Loukeris TG, Paine MJ. 2006. *Anopheles gambiae* P450 reductase is highly expressed in oenocytes and in vivo knockdown increases permethrin susceptibility. *Insect Mol Biol* 15:321-7

Lumjuan N, McCarrol L, Prapanthadara L, Hemingway J, Ranson H. 2005. Elevated activity of an Epsilon class glutathione transferase confers DDT resistance in the dengue vector, *Aedes aegypti*. *Insect Biochem Mol Biol* 35:861-871

Lumjuan N, Rajatileka S, Changsom D, Wicheer J, Leelapat P, Prapanthadara LA, Somboon P, Lycett G, Ranson H. 2011. The role of the *Aedes aegypti* Epsilon glutathione transferases in conferring resistance to DDT and pyrethroid insecticides. *Insect Biochem Mol Biol* 41:203-209

Lümmen P. 2007. Mitochondrial electron transport complexes as biochemical target sites for insecticides and acaricides. In: Ishaaya I, Nauen R, Horowitz AR. (Eds.), Insecticides Design Using Advanced Technologies. Springer Verlag, Berlin, Heidelberg 197-215

Martinez-Torres D, Foster SP, Field LM, Devonshire AL, Williamson MS. 1999. A sodium channel point mutation is associated with resistance to DDT and pyrethroid insecticides in the peach-potato aphid, *Myzus persicae* (Sulzer) (Hemiptera : Aphididae). *Insect Mol Biol* 8:339-346

McKellar QA, Benchaoui HA. 1996. Avermectins and milbemycins. *J Vet Pharmacol Ther* 19:331-351

Mermans C, Dermauw W, Geibel S, Van Leeuwen T. 2017. A G326E substitution in the glutamate-gated chloride channel 3 (CluCl3) of the two-spotted spider mite *Tetranychus urticae* abolishes the agonistic activity of macrocyclic lactones. *Pest Manag Sci* 73:2413-2418

Migeon A, Dorkeld F. 2010. Spider Mites Web: a Comprehensive Database for the Tetranychidae. http://www.montpellier.inra.fr/CBGP/spmweb

Mills LR. 1973. Structure of dorsal setae in the two-spotted spider mite *Tetranychus urticae* Koch, 1836. *Acarol* 15:649-658

Nauen R, Wolfel K, Lueke B, Myridakis A, Tsakireli D, Roditakis E, Tsagkarakou A, Stephanou E, Vontas J. 2015. Development of a lateral flow test to detect metabolic resistance in Bemisia tabaci mediated by CYP6CM1, a cytochrome P450 with broad spectrum catalytic efficiency. *Pestic Biochem Phys* 121:3:11

Nebert DW. 1991. Proposed role of drug-metabolizing enzymes: Regulation of steady state levels of the ligands that effect growth, homeostasis, differentiation, neuroendocrine functions. *Mol. Endocrinol.*, *5*:1203–1214

Nelson DR. 1998. Metazoan cytochrome P450 evolution. *Comp. Biochem. Physiol. C Pharmacol. Toxicol. Endocrinol. 121*:15–22

Nelson DR, Kamataki T, Waxman DJ, Guengerich FP, Estabrook RW. et al. 1993. The P450 superfamily: Update on new sequences, gene mapping, accession numbers, early trivial names of enzymes, nomenclature. *DNA Cell. Biol.*, *12*:1–51

Nelson DR, Koymans L, Kamataki T, Stegeman JJ, Feyereisen R. et al. 1996. P450 superfamily: Update on new sequences, gene mapping, accession numbers and nomenclature. *Pharmacogenetics*, *6*:1–42

Nicastro RL, Sato ME, Da Silva MZ. 2010. Milbemectin resistance in *Tetranychus urticae* (Acari: Tetranychidae): selection, stability and cross-resistance to abamectin. *Expl Appl Acarol* 50(3):231-241

Nikou D, Ranson H, Hemingway J. 2003. An adult-specific CYP6 P450 gene is over-expressed in apyrethroid-resistant strain of the malaria vector, *Anopheles gambiae*. *Gene* 318:91-102

Omura T, Sato R. 1964. The carbon monoxide-binding pigment of liver microsomes I. Evidence for its hemoprotein nature. *J. Biol. Chem.*, *239*:2370–2378

Park YL, Lee JH. 2002. Leaf cell and tissue damage of cucumber caused by two spotted spider mite (Acari:Tetranychidae). *J Econ Entomol* 95:952–957

Pavlidi N, Khalighi M, Myridakis A, Dermauw W, Wybouw N, Tsakireli D, Stephanou EG, Labrou NE, Vontas J, Van Leeuwen T. 2017. A glutathione-S-transferase (TuGSTd05) associated with acaricide resistance in *Tetranychus urticae* directly metabolizes the complex II inhibitor cyflumetofen, *Insect Biochemistry and Molecular Biology* doi: 10.1016/j.ibmb.2016.12.00

Pavlidi N, Tseliou V, Riga M, Nauen R, Van Leeuwen T, Lambrou NE, Vontas J. 2015. Functional characterization of glutathione S-transferases associated with insecticide resistance in *Tetranychus urticae*. *Pest Biochem Physiol* 121:53-60

Pedigo LP. 1989. Entomology and pest management.

Plapp FW Jr, Hoyer RF. 1968. Insecticide resistance in the house fly: decreased rate of absorption as a mechanism of action of a gene that acts as an intensifier of resistance. *J Econ Entomol* 61:1298-1303

Puinean AM, Foster SP, Oliphant L, Denholm I, Field LM, Millar NS, Williamson MS, Bass C. 2010. Amplification of a Cytochrome P450 Gene Is Associated with Resistance to Neonicotinoid Insecticides in the Aphid *Myzus persicae*. *PLoS Genetics* 6:e1000999

Putter I, Mac Connell JG, Preiser FA, Haidri AA, Ristich SS, Dybas RA. 1981. Avermectins: novel insecticides, acaricides and nematicides from soil microorganism. *Experientia* 37:963-964

Ranson H, Rossiter L, Ortelli F, Jensen B, Wang X, Roth CW, Collins FH, Hemingway J. 2001. Identification of a novel class of insect glutathione S-transferases involved in resistance to DDT in the malaria vector *Anopheles gambiae*. *Biochem J* 359:295-304

Reddy BPN, Prasad GBKS, Raghavendra K. 2011. In silico analysis of glutathione S-transferase supergene family revealed hitherto unreported insect specific delta- and epsilon-GSTs and mammalian specific mu-GSTs in *Ixodes scapularis* (Acari: Ixodidae). *Comput Biol Chem* 35(2):114–20

Riga M, Myridakis A, Tsakireli D, Morou E, Stephanou EG, Nauen R, Van Leeuwen T, Douris V, Vontas J. 2015. Functional characterization of the *Tetranychus urticae* CYP392A11, a cytochrome P450 that hydroxylates the METI acaricides cyenopyrafen and fenpyroximate. *Insect Biochem Molecul Biol* 65:91-99

Riga M. PhD. 2016. Molecular, Genetic and functional characterization of pesticide resistance mechanisms of *Tetranychus urticae*. University of Crete. Department of Biology

Riga M, Tsakireli D, Ilias A, Morou E, Myridakis A, Stefanou EG, Nauen R, Dermauw W, Van Leeuwen T, Paine M, Vontas J. 2014. Abamectin is metabolized by CYP392A16, a cytochrome P450 associated with high levels of acricide resistance in *Tetranychus urticae*. *Insect Biochem Mol Biol* 46:43-53

Rosenheim JA, Johnson MW,Mau RFL, Welter SC, Tabashnik BE. 1996. Biochemical preadaptations, founder events, and the evolution of resistance in arthropods. *J. Econ. Entomol.* 89:263–73

Russell TL, Govella NJ, Azizi S, Drakeley CJ, Kachur SP, Killeen GF. 2011. Increased proportions of outdoor feeding among residual malaria vector populations following increased use of insecticide-treated neta in rural Tazmania. *Malar J* 10:80

Salinas AE, Wong MG. 1999. Glutathione S-transferases-A review. *Curr Medic Chem* 6:279-309

Sances FV, Wyman JA, Ting IP. 1979. Morphological responses of strawberry leaves to infestations of two spotted spider mite. *J Econ Entomol* 72:710–713

Seixas G, Grigoraki L, Weetman D, Vicente JL, Silva AC, Pinto J, … Sousa CA. 2017. Insecticide resistance is mediated by multiple mechanisms in recently introduced *Aedes aegypti* from Madeira Island (Portugal). *PLoS Negl Trop Diseas* 11 (7):e0005799

Silver KS, Du Y, Nomura Y, Oliveira EE, Salgado VL, Zhorov BS, Dong K. 2014. Voltage-gated sodium channels as insecticide target sites. *Advan Insec Physiol* 46:389-433

Small G, Hemingway J. 2000. Molecular characterization of the amplified carboxylesterase gene associated with organophosphorus insecticide resistance in the brown planthopper , *Nilaparvata lugens*. *Insect Mol Biol* 9:647-653

Sonoda S, Igaki C, Tsumuki H. 2008. Alternatively spliced sodium channel transcripts expressed in field strains of the diamondback moth. *Ins Biochem Molec Biol* 38:883-890

Sparks TC, Lockwood JA, Byford RL, Graves JB, Leonard BR. 1989. The role of behavior in insecticide resistance. *Pestic Sci* 26:383-399

Sparks TC, Nauen R. 2014. IRAC: Mode of action classification and insecticide resistance management. *Pest Biochem Physiol* 121:122-128

Sugimoto N, Osakabe M. 2014. Cross-resistance between cyenopyrafen and pyridaben in the twospotted spider mite *Tetranychus urticae* (Acari: Tetranychidae). *Pest Manag Sci* 70(7):1090-1096

Takahashi N, Nakagawa H, Sasama Y, Ikemi N. 2012. Development of a new acaricide, cyflumetofen. *J Pestic Sci* 37:263-264

Tsagkarakou A, Van Leeuwen T, Khajehali J, Ilias A, Grispou M, Williamson MS, Tirry L, Vontas J. 2009. Identificaion of pyrethroid resistance associated mutations in the *para* sodium channelof the two-spotted spider mite *Tetranychus urticae* (Acari:Tetranychidae). *Insect Mol Biol* 18:583-593

Tew KD. 1994. Glutathione-associated enzymes in anticancer drug resistance. *Cancer Res* 54:4313–4320

Vaillancourt FH, Bolin JT, Eltis LD. 2008. The ins and outs of ring-cleaving dioxygenases. *Crit Rev Biochem Mol Biol* 41:241-267

Van Leeuwen T, Dermauw W. 2016. The molecular evolution of xenobiotic metabolism and resistance in chelicerate mites. *Annu Rev Entomol* 61:475-498

Van Leeuwen T, Vanholme B, Van Pottelberge S, Van Nieuwenhuyse P, Nauen R, Tirry L, Denholm I. 2008. Mitochondrial heteroplasmy and the evolution of insecticide resistance: non-Mendelian inheritance in action. *Proc Natl Acad Sci USA* 105:5980-5985

Van Leeuwen T, Vontas J, Tsagkarakou A. 2009. Mechanisms of acaricide resistance in the two spotted spider mite Tetranychus urticae. Ishaaya, I, Horowitz AR. (Eds.), Biorational Control of Arthropod Pests. Springer, The Netherlands, pp 347-393

Van Pottelberge S. 2008. Mechanisms and impact of acaricide resistance in strains of *Tetranychus urticae*: a genetic, biochemical and biological approach. Ghent University, Faculty of Bioscience engineering.

Vetting MW, Ohlendorf DH. 2000. The 1.8 °A crystal structure of catechol 1,2-dioxygenase reveals a novel hydrophobic helical zipper as a subunit linker. *Structure* 8:429–440

Vontas JG, Small GJ, Nikou DC, Ranson H, Hemingway J. 2002. Purification, molecular cloning and heterologous expression of a glutathione S-transferase involved in insecticide resistance from the rice brown planthopper, *Nilaparvata lugens*. *Biochem J* 362:329-337

Wang Y, Qiu L, Ranson H, Lunjuan N, Hemingway J, Setzer WN, Meehan EJ, Chen L. 2008. Structure of an insect epsilon class glutathione S-transferase from the malaria vector *Anopheles gambiae* provides an explanation for the high-DDT detoxifying activity. *J Struct Biol* 164:228-235

Wei SH, Clark AG, Syvanen M. 2001. Identification and cloning of a key insecticide-metbolizing glutathione S-transferase (MdGST-6A) from a hyper insecticide-resistant strain of the house fly *Musca domestica*. *Insect Biochem Mol Biol* 31:1145-1153

Werck-Reichhart D, Feyereisen R. 2000. Cytochromes P450: a success story. *Genome Biol* 1: 1-9

Wilce MCJ, Parker MW. 1994. Structure and function of glutathione S-transferases. *Biochem Biophys Acta* 1205:1-18

Williamson MS, Martinez-Torres D, Hick CA, Devonshire AL. 1996. Identification of mutations in the housefly para-type sodium channel gene associated with knockdown resistance (kdr) to pyrethroid insecticides. *Molecul Gener Genet* 252:51-60

Winayanuwattikun P, Ketterman AJ. 2005. An electron-sharing network involved in the catalytic mechanism is functionally conserved in different glutathione transferase classes. *Jour biol chem* 280: 31776-31782

Wolstenholme AJ, Rogers AT. 2005. Glutamate-gated chloride channels and the mode of action of the avermectin/milbemycin anthelmintics. *Parasitology* 131:85-95

Xuan N, Guo X, Xie HY, Lou QN, Lu XB, Liu GX, Picimbon JF. 2015. Increased expression of CSP and CYP genes in adult silkworm females exposedto avermectins. *Insect Sci* 00:1-17

Yahouédo GA, Chandre F, Rossignol M, Ginibre C, Balabanidou V, Mendez NGA, Pigeon O, Vontas J, Cornelie S. 2017. Contributions of cuticle permeability and enzyme detoxification to pyrethroid resistance in the major malaria vector *Anopheles gambiae*. *Sci Rep* 7:11091

Yang J, McCart C, Woods DJ, Terhazaz S, Greenwood KG, ffrench-Constant RH, Dow LA. 2007. A drosophila systems approach to xenobiotic metabolism. *Physiol Genomics* 30:223-231

Yu H, Xu M, Cheng Y,Wu H, Luo Y, Li B. 2012. Synthesis and acaricidal activity of cyenopyrafen and its geometric isomer. Arkivoc vi, 26-34

Zalucki MP, Furlong MJ. 2017. Behavior as a mechanism of insecticide resistance: evaluation of the evidence. *Curr Opin Insect Sci* 21:19-2

Zhang K, Niu JZ, Ding TB, Dou W, Wang JJ. 2013. Molecular characterization of two carboxylesterase genes of the citrus red mite, *Panonychus citri* (Acari:Tetranychidae). *Arch Insect Biochem Physiol* 82:213-226

Zhang L, Gao X, Liang P. 2007. Beta-cypermethrin resistance associated with high carboxylesterase activities in a strain of house fly *Musca domestica* (Diptera: Muscidae). *Pest Biochem Physiol* 89:65-72

Zhang S, Zhang X, Shen J, Li D, Wan H, You H, Li J. 2017. Cross-resistance and biochemical mechanisms of resistance to indoxcarb in the diamondback moth *Plutella xylostella*. *Pestic Biochem Physiol* 140:85-89

Zhou D, Duan B, Sun Y, Ma L, Zhu C, Shen B. 2017. Preliminary characterization of putative structural cuticular proteins in the malaria vector *Anopheles sinensis. Pest Manag Sci* 73:2519-2528

Zhu F, Parthasarathy R, Bai H, Woithe K, Kaussmann M, Nauen R, … Palli SR. 2010. A brain-specific cytochrome P450 responsible for the majority of deltamethrin resistance in the QTC279 strain of *Tribolium castaneum*. *Proceed Nation Acad Sci USA 107*(19):8557–8562